GE Energy

David H. Hinds
Manager, ESBWR

PO Box 780 M/C L60
Wilmington, NC 28402-0780
USA

T 910 675 6363
F 910 362 6363
david.hinds@ge.com

MFN 06-348

Docket No. 52-010

September 29, 2006

U.S. Nuclear Regulatory Commission
Document Control Desk
Washington, D.C. 20555-0001

Subject: **Response to Portion of NRC Request for Additional Information Letter No. 33 Related to ESBWR Design Certification Application – Engineered Safety Features – RAI Numbers 6.2-52, and 6.2-58**

Enclosure 1 contains GE's response to the subject NRC RAI transmitted via the Reference 1 letter.

If you have any questions about the information provided here, please let me know.

Sincerely,

George Strambac for

David H. Hinds
Manager, ESBWR

D068

Reference:

1. MFN 06-167, Letter from U.S. Nuclear Regulatory Commission to David Hinds, *Request for Additional Information Letter No. 33 Related to ESBWR Design Certification Application,* June 1, 2006

Enclosure:

MFN 06-348 – Response to Portion of NRC Request for Additional Information Letter No. 33 Related to ESBWR Design Certification Application – Engineered Safety Features – RAI Numbers 6.2-52, and 6.2-58

cc: AE Cubbage USNRC (with enclosures)
GB Stramback GE/San Jose (with enclosures)
eDRF 0057-1236, 0057-1325, 0058-4485

MFN 06-348

ENCLOSURE 1

Response to Portion of NRC Request for

Additional Information Letter No. 33

Related to ESBWR Design Certification Application

Engineered Safety Features

RAI Numbers 6.2-52, and 6.2-58

NRC RAI 6.2-52

The TRACG model used for DCD analyses does not include the "tee" model used to control the release of non-condensable gases from the lower drywell. The approved approach addressed uncertainties in TRACG's ability to account for mixing and stratification in the drywell.

A. In the evaluation of the main steam line break (MSLB), was the preapplication model used or was the newer DCD version of the TRACG model used? Include this information in the DCD Tier 2.

B. If the new model was used, provide justification for its use in licensing analyses for MSLBs, specifically address noncondensable gas holdup, mixing and stratification. Include this information as an update to NEDC-33083P-A, "TRACG Application for ESBWR."

C. If the new model is used for the MSLB, provide a discussion of the containment response to the MSLB using this model, particularly with respect to the movement of noncondensable gases, mixing and stratification, throughout the containment, and relate the response to the preapplication model. Include this information as an update to NEDC-33083P-A, "TRACG Application for ESBWR."

GE Response

Response to RAI 6.2-52 A

The newer DCD version of the TRACG model (shown in Figures 6.2-6 to 6.2-8, DCD Tier 2, Rev. 1) was used in the evaluation of the main steam line break (MSLB) presented in the DCD Tier 2, Rev. 1.

DCD Section 6.2.1.1.3 (Page 6.2-13, DCD Tier 2, Rev. 1) will be revised in the next update to include the above discussion.

Response to RAI 6.2-52 B

Tie-back calculations were performed with the combined TRACG nodalization similar to that presented in the DCD Tier 2, Rev. 1. The results for these calculations were compared with those using the TRACG nodalizations presented in the NEDC-33083P-A report. These tie-back calculations include a total of three cases used in the NEDC-33083P-A report, two for the ECCS analysis (short-term calculation) and one for the containment analysis (long-term calculation). Results of this comparison show that the calculations using the combined TRACG nodalization compared well with those from the base cases, and the impacts due to nodalization changes on the minimum chimney static head level (+0.1 to -0.16 m) and on the long-term drywell pressure (< 0.3 psia) are judged to be small by comparing to the margins.

The following paragraphs discuss the results of these tie-back calculations, including the effect on the non-condensable (NC) gases holdup, mixing and stratification.

These discussions will be included in the Supplement in DCD Section 6.2.

Combined Nodalization

In the TRACG Application Report (NEDC-33083P-A report), two nodalizations are used for the calculations, Figure 6.2-52_1 (from Figure 2.7-1 in NEDC-33083P-A) for the ECCS analyses (short-term) and Figure 6.2-52_2 (from Figure 3.7-1 in NEDC-33083P-A) for the Containment (long-term) analyses. In the SER on NEDC-33083P, several subjects regarding these two nodalizations are included as Confirmatory Items in the NEDC-33083P-A report. A combined nodalization for use in both the short-term and the long-term calculations is desirable for the ESBWR licensing analyses. This combined nodalization addresses the confirmatory items in the NEDC-33083P-A report. (DCD Tier 2, Rev. 1, Table 6.2-6a)

The combined nodalization merges the detailed RPV model in Figure 6.2-52_1 with the detailed containment model in Figure 6.2-52_2. For comparison purpose, the combined nodalization is developed in two steps. In the first step, the component TEE35 is used to model the lower drywell. And in the second step, component TEE35 is replaced with additional vessel levels and cells to model the lower drywell.

Model COMB-5 (with TEE35 to model the Lower Drywell)

Figure 6.2-52_3 shows the combined nodalization in the first step (Model COMB-5, with TEE35 as the Lower Drywell). The vessel component in this model has a total of 39 axial levels and 8 rings.

Cells in VSSL Levels 1 to 21, Rings 1 to 4 in Model COMB-5 are used to model the RPV, identical to that as shown in Figure 6.2-52_1 (RPV portion). Cells in Levels 1 to 21, Rings 5 to 8 in Model COMB-5 are dummy cells or dead cells. These cells are not participated in the calculation.

Cells in VSSL Levels 22 to 32, Rings 1 to 4 in Model COMB-5 are dummy cells or dead cells. Cells in Levels 22 to 32, Rings 5 to 8 in Model COMB-5 are used to model the drywell, suppression pool, wetwell, and GDCS pool. These VSSL cell inputs are converted from those containment cells in Levels 1 to 11, Rings 3 to 6, shown in Figure 6.2-52_2.

Cells in VSSL Levels 33 to 39, Rings 1 to 2 in Model COMB-5 are dummy cells or dead cells. Cells in Levels 33 to 39, Rings 3 to 8 in Model COMB-5 are used to model the PCC/IC pool. These VSSL cell inputs are converted from those containment cells in Levels 12 to 18, Rings 1 to 6, shown in Figure 6.2-52_2.

The one-dimensional TRACG components in COMB-5 are converted from those in Figure 6.2-52_1 and Figure 6.2-52_2. The drain tanks (TEE62 and TEE46) in Figure 6.2-52_2 are not shown in Figure 6.2-52_3.

Model COMB-6 (with VSSL Cells to model the Lower Drywell)
Figure 6.2-52_4 shows the combined nodalization in the second step (Model COMB-6), replacing component TEE35 with additional vessel levels and cells to model the lower drywell. The vessel component in this model has a total of 42 axial levels and 8 rings, 3 more axial levels than that in Model COMB-5.

VSSL Levels 1 to 21 in COMB-6 are identical to those in COMB-5. VSSL Levels 22 and 23, Rings 1 to 6, are used to model the lower drywell. The total volume in these cells is calculated to be the same as that in TEE035. Cells in Levels 24 to 34, Ring 5 to 8 in Model-6 are used to model the drywell, wetwell, suppression pool, and GDCS pools. These cells are converted from those in COMB-5, Levels 21 to 31.

In COMB-6, one additional axial (Level 31) is added at a location close to the top of wetwell. The main purpose of this additional axial layer is to simulate the thin layer near the top of the wetwell. The NC gases trapped inside this thin layer (between the I-beams) will have restricted flow paths and therefore more thermal stratification. Axial Level 35, Cells 1 to 4 are used to model the DW head airspace. Axial Level 35, Cells 7 to 8 are used to model a small airspace above the GDCS pool. The connection PIPE81 and PIPE82 connect this level and Level 31 (top of WW).

Cells in Levels 36 to 42, Rings 3 to 8 in Model COMB-6 are used to model the PCC/IC pool, same as those in Level 33 to 39 in Model COMB-5.

The one-dimensional TRACG components in COMB-6 are same as those in COMB-5. The drain tanks (TEE62 and TEE46) in Figure 6.2-52_2 are not shown in Figure 6.2-52_4.

Tie-Back Calculations

The baseline case (nominal main steam line break, MSLB-NL2_V40) discussed in Section 3.7.2 in "TRACG Application for ESBWR, NEDC-33083P-A, is calculated using the combined nodalizations COMB-5 and COMB-6. The initial conditions and thermo-hydraulic conditions in the cells (such as volume, pressure, temperature, etc.) are consistent among these cases: MSLB-NL2_V40, MSLB-CB5 and MSLB-CB6. All these cases are run using the 9-Apr-2004 Version of the TRACG04 (ALPHA Version). Results from these calculations are discussed and compared in the following paragraphs.

Comparison between MSLB-CB5 and MSLB-NL2_V40 (0 – 72 hr)

Figure 6.2-52_5 shows the GDCS pool and downcomer water levels for Case "MSLB-CB5", and Figure 6.2-52_6 shows the GDCS pool and downcomer water levels for Case

"MSLB-NL2_V40". For Case "MSLB-NL2_V40", the RPV is modeled by 11 axial levels and 2 rings (Figure 6.2-52_2). The downcomer level response for this Case (Figure 6.2-52_6) is more exaggerated because of the coarse nodalization for the RPV. The downcomer level response for Case "MSLB-CB5" (Figure 6.2-52_5) is milder and smoother due to finer nodalization for the RPV (21 axial levels and 4 rings).

Figure 6.2-52_7 compares the total PCC condensation powers between these two Cases. For "MSLB-NL2_V40", because of the exaggerated DC level response, the condensation power shows spiky drops at the time of the spiky increases in the DC level (Figure 6.2-52_6). The additional subcooled water in the downcomer consumes part of the decay energy and reduces the production of steam that is feeding the PCCS. For the first 9 hrs, the total condensation power for Case "MSLB-CB5" is slightly less than that for Case "MSLB-NL2_V40". The difference in energy between the decay heat and the total PCC power is discharged into the suppression pool and heats up the pool water. In this case, Case "MSLB-CB5" discharges more energy to the suppression pool. This is the consequence of more accurate nodalization of the RPV. The total PCC condensation power is greater than the decay heat after 9 ~ 10 hours. From that time on, the added energy to the suppression pool water due the movement of NC gases from the DW to the WW is not significant because of the over-capacity in the PCCS.

Figure 6.2-52_8 compares the suppression pool water temperature at the surface. For both cases, the pool surface temperatures increase during the first 9 hrs. However, the pool surface temperature for Case "MSLB-CB5" is higher than that for Case "MSLB-NL2_V40" by about 8 °F at the end of 9 hr (because the PCCS condensation power is lower for the Case "MSLB-CB5").

Figure 6.2-52_9 shows the Drywell partial NC gas pressures for Case "MSLB-CB5", and Figure 6.2-52_10 shows the Drywell partial NC gas pressures for Case "MSLB-NL2_V40". During the first 18 hours, Case "MSLB-CB5" retains more NC gases in the DW than that for Case "MSLB-NL2-V40". It takes 54 hours to purge all DW NC gases for Case "MSLB-CB5", while it takes 48 hours for Case "MSLB-NL2-V40". The long-term NC gas distribution depends on the NC gas circulation pattern, which depends on the DW annulus geometry and the strength of the steam source. However the difference in purged timing has no significant impact on the long-term DW pressure (Figure 6.2-52_11).

Figure 6.2-52_11 compares the DW pressures between these two Cases. During the first 9 hours, the DW pressure for Case "MSLB-NL2_V40" is higher than that for Case "MSLB-CB5", due to lesser NC gases remaining in the DW. After all the NC gases have been purged into the WW (48 hrs for Case "MLSB-NL2_V40", 54 hrs for Case "MSLB-CB5"), the DW pressures reach the maximum value for the rest of the transient. The maximum DW pressure for Case "MSLB-CB5" is 1.3 psia higher than that for Case "MSLB-NL2-V40", corresponding to the higher suppression pool surface temperature in Case "MSLB-CB5" (Figure 6.2-52_8).

Comparison between MSLB-CB6 and MSLB-CB5 (0 – 72 hr)

Figure 6.2-52_9 shows the Drywell partial NC gas pressures for Case "MSLB-CB5", and Figure 6.2-52_12 shows the Drywell partial NC gas pressures for Case "MSLB-CB6". During the first 18 hours, Case "MSLB-CB5" retains more NC gases in the DW than that for Case "MSLB-CB6". It takes 54 hours to purge all DW NC gases for Case "MSLB-CB5", while it takes 21 hours for Case "MSLB-CB6". The DW pressure reaches the maximum value when all the NC gases have been purged in the WW (Figure 6.2-52_14). The difference in the timing for purging all NC gases shows no impact on the peak value.

Figure 6.2-52_13 compares the RPV, DW and WW pressures for Case "MSLB-CB6". After all the NC gases have been purged into the WW (21 hrs for Case "MSLB-CB6"), the DW pressure reaches the maximum value for the rest of the transient. There are 12 VB openings between 21 and 72 hours, as shown in Figures 6.2-52_12 and 6.2-52_13. Small amount of NC gases are cycling back and forth between the DW and WW. These VB openings have no impact on the peak DW pressure (Figure 6.2-52_14).

Figure 6.2-52_14 compares the DW pressures between Cases "MSLB-CB6", "MSLB-CB5" and "MSLB-NL2_V40". After all the NC gases have been purged into the WW (48 hrs for Case "MSLB-NL2_V40", 54 hrs for Case "MSLB-CB5", and 21 hrs for Case "MSLB-CB6"), the DW pressures reach the maximum value for the rest of the transient. The maximum DW pressure for Case "MLSB-CB5" is higher than that for Case "MSLB-NL2_V40", corresponding to the higher suppression pool surface temperature in Case "MSLB-CB5" (Figure 6.2-52_8). The maximum DW pressure for Case "MSLB-CB6" is 0.3 psia lower than that for Case "MSLB-CB5", when all NC gases have been purged into the WW.

Figure 6.2-52_15 shows the suppression pool temperatures for Case "MSLB-CB6", and Figure 6.2-52_16 shows the suppression pool temperatures for Case "MSLB-CB5". The peak pool temperature for Case "MSLB-CB6" is about 1 °F lower than that for Case "MSLB-CB5".

Figure 6.2-52_17 shows the PCC condensation power for Case "MSLB-CB6", and Figure 6.2-52_18 shows the PCC condensation power for Case "MSLB-CB5". For Case "MSLB-CB6", there are 12 spikes in the total PCC condensation power between 21 and 72 hours, corresponding to the VB openings. The PCC condensation powers between Cases "MSLB-CB5" and "MSLB-CB6" agree well as shown in these figures.

Summary

Main steam line breaks were simulated using the combined nodalization (with and without the TEE35 as the lower DW).

The downcomer level response for the cases using the combined nodalization is milder and more accurate compared to the base case, which is exaggerated because of the coarse nodalization for the RPV. The suppression pool surface temperature is about 8 °F higher than that for the base case, due to slightly more energy discharging to the suppression

pool during the first 9 hrs. The long-term DW pressure is about 1.3 psia higher than that in the base case, due to higher suppression pool surface temperature.

Modeling the lower DW with VSSL cells leads to shorter time period (21 hours for VSSL cells versus 54 hours for TEE35) for purging all drywell NC gases into the WW. However, the effect of purging time period on the peak, long-term DW pressure is small and is less than 0.3 psia (Figure 6.2-52_14). The relatively small effect is due to that the total PCC condensation power is greater than the decay heat after 9 ~ 10 hours. From that time on, the added energy to the suppression pool water due the movement of NC gases from the DW to the WW is not significant because of the over-capacity in the PCCS. The DW pressure reaches the maximum value when all the NC gases have been purged in the WW (Figure 6.2-52_14). The difference in the timing for purging all NC gases and the subsequent V/B openings show no significant impact on the peak value.

Results of this comparison show that the calculations using the combined TRACG nodalization compared well with those from the base cases, and the impacts due to nodalization changes on the minimum chimney static head level (+0.1 to -0.16 m) and on the long-term drywell pressure (< 0.3 psia) are judged to be small by comparing to the margins.

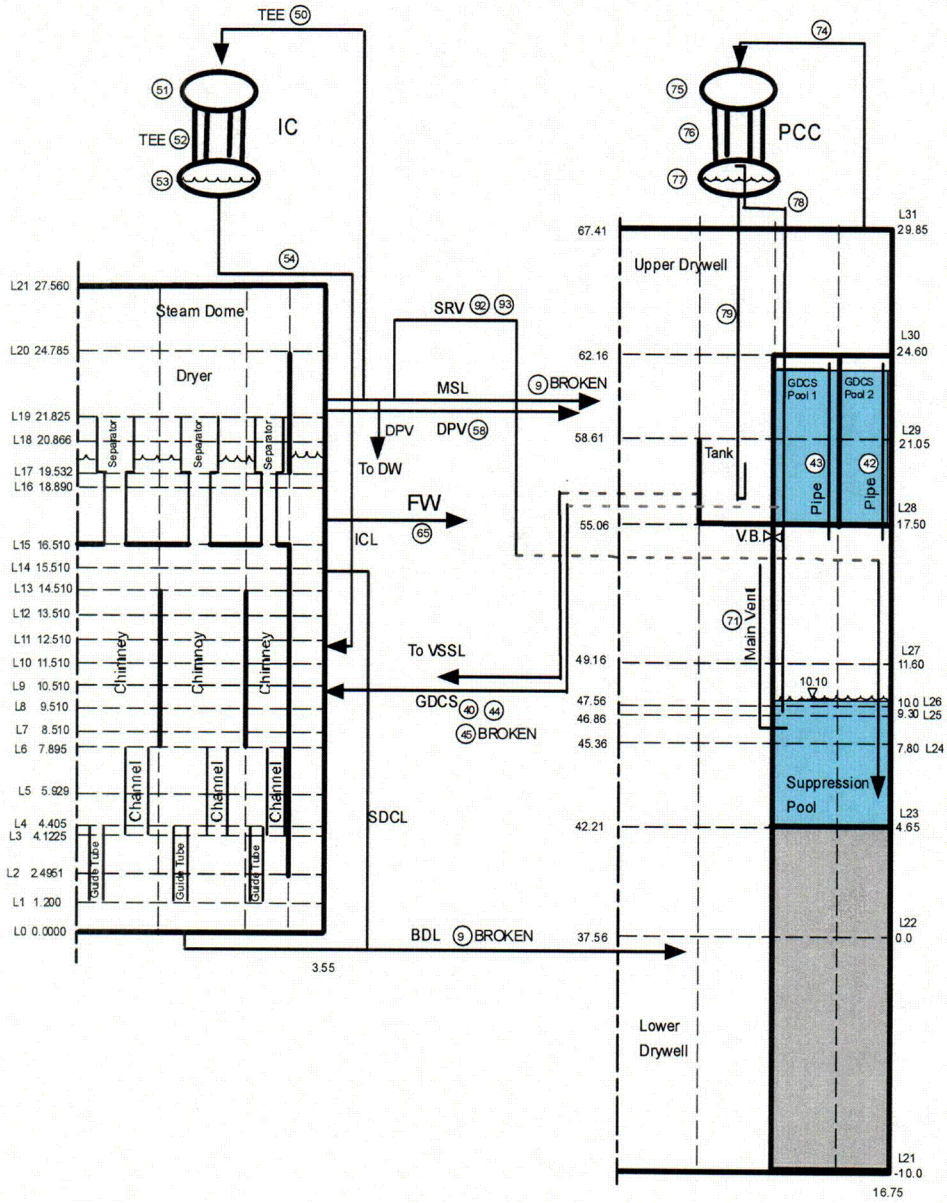

ESBWR TRACG LOCA MODEL

ESBWR1-b.CNV

Figure 6.2-52_1 TRACG Nodalization for ESBWR ECCS/LOCA Analysis (NEDC-33083P-A)

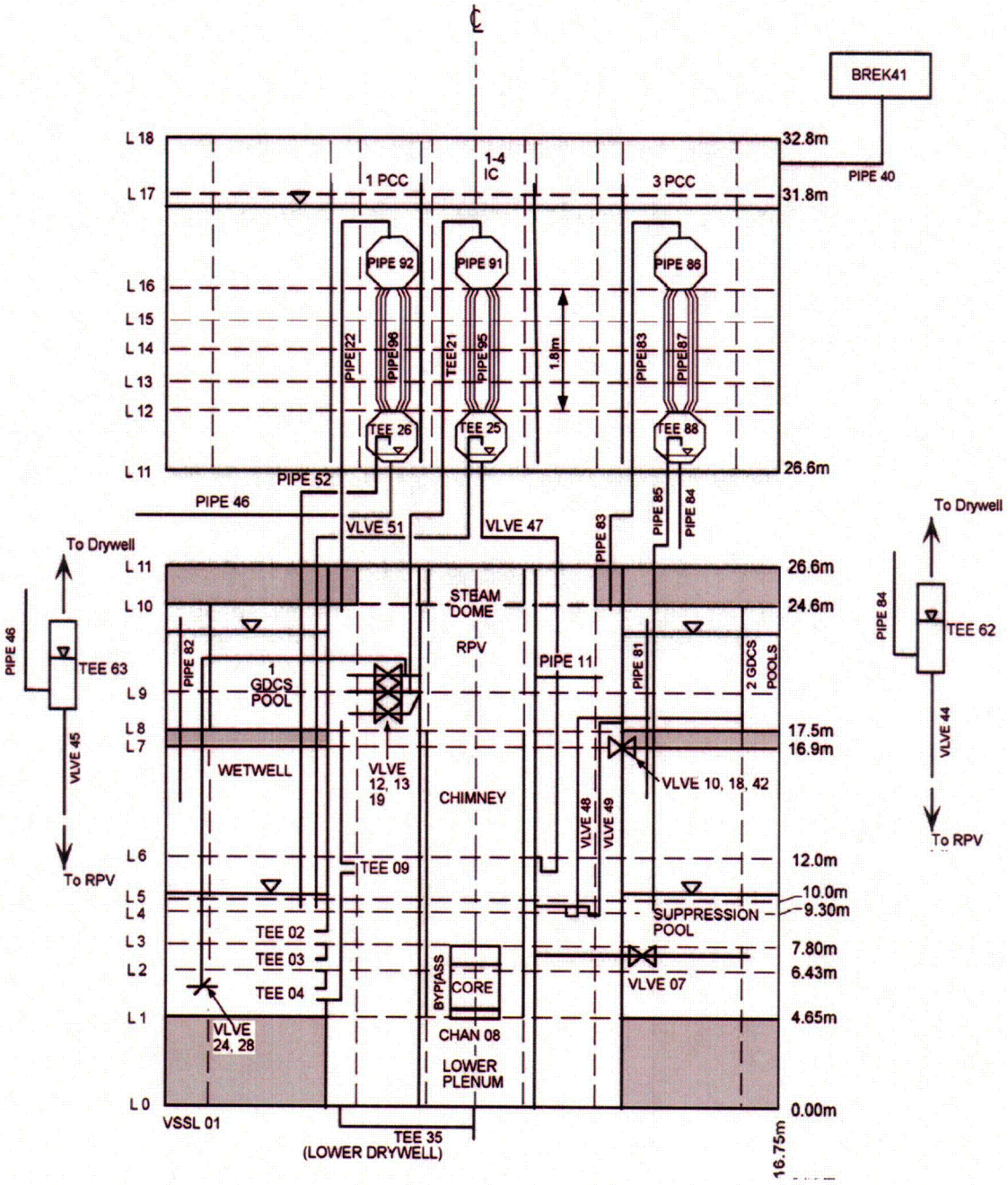

Figure 6.2-52_2 TRACG Nodalization for ESBWR Containment Analysis (NEDC-33083P-A)

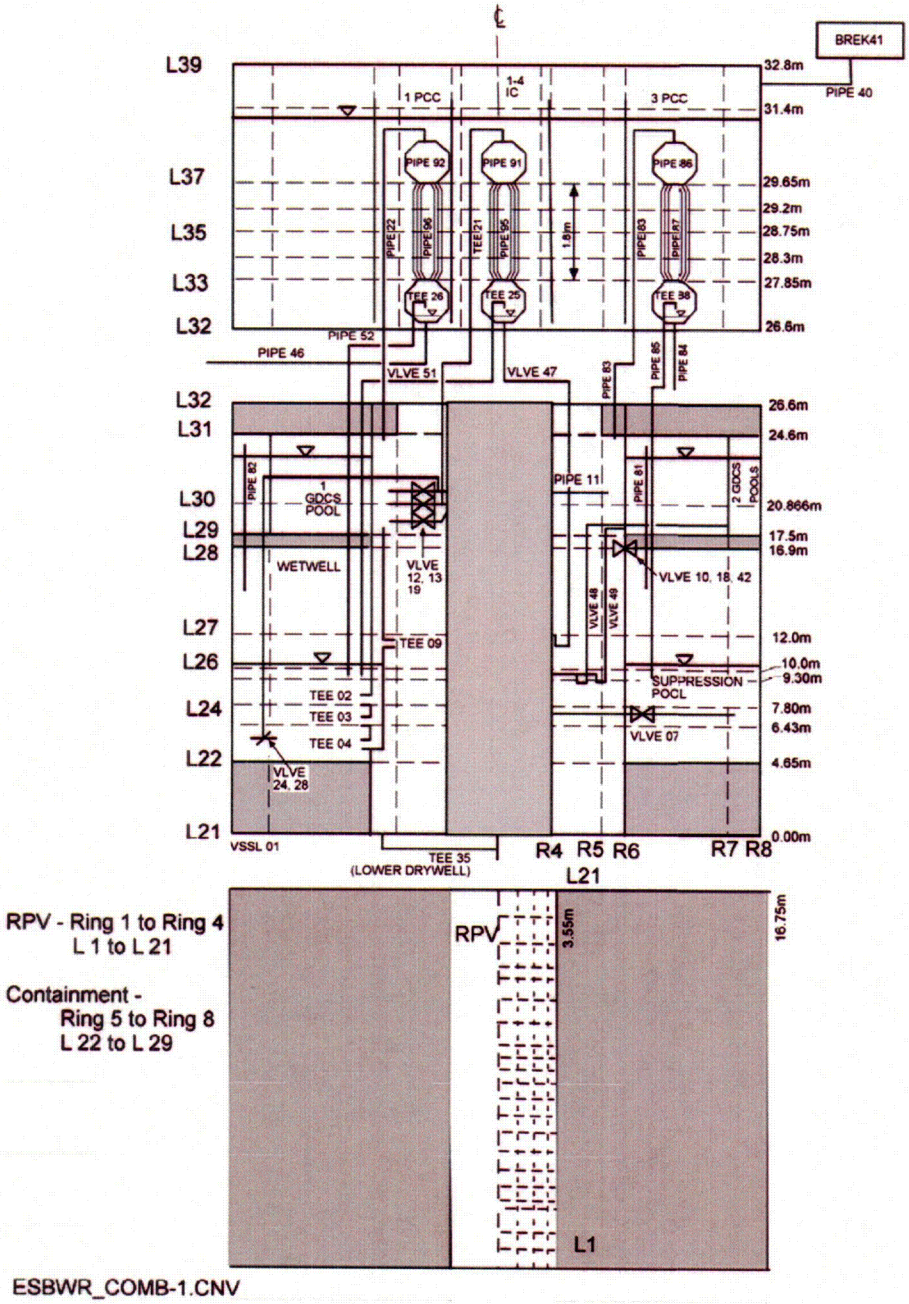

Figure 6.2-52_3 TRACG Combined Nodalization
(Model COMB-5, with TEE35 as Lower Drywell)

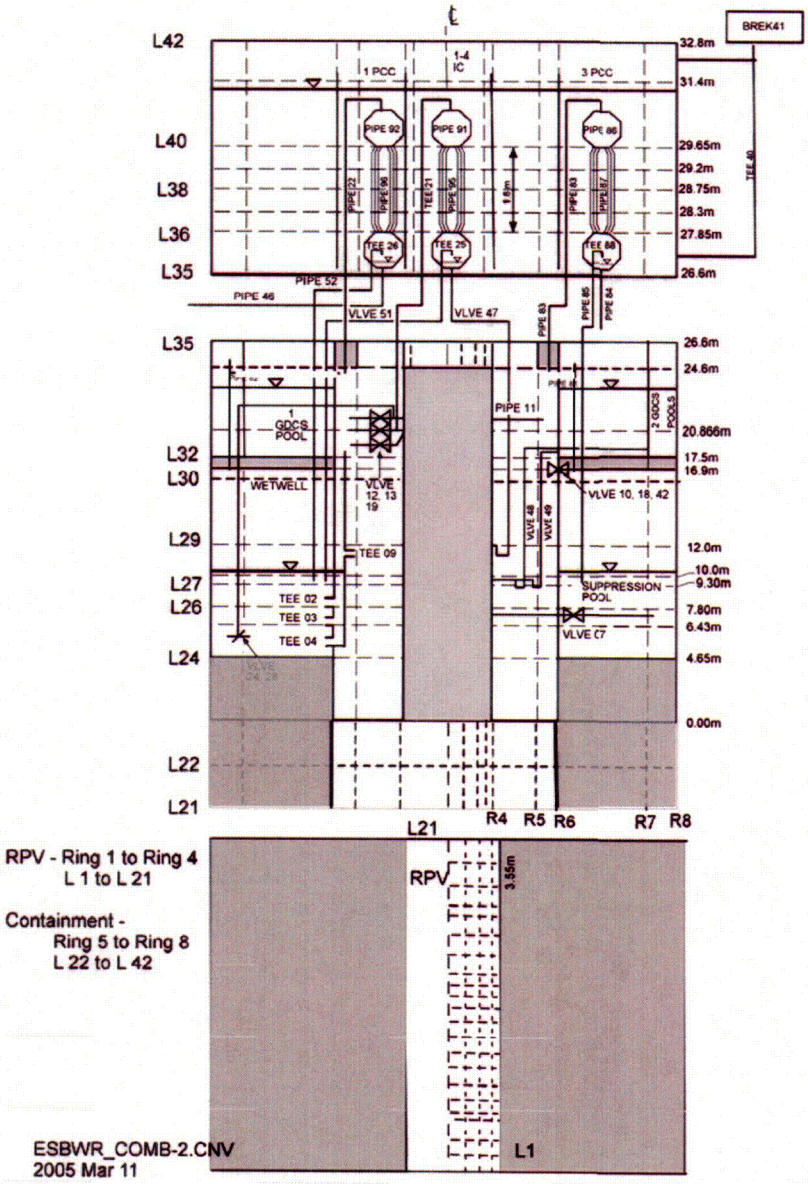

Figure 6.2-52_4 TRACG Combined Nodalization
(Model COMB-6, without TEE35 as Lower Drywell)

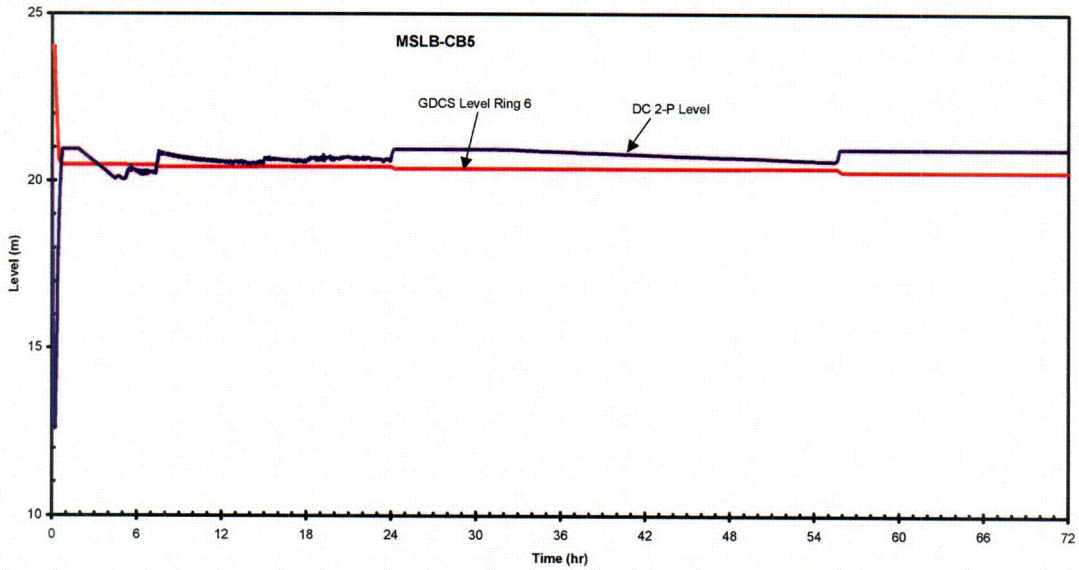

Figure 6.2-52_5 MSLB-CB5 – GDCS and DC Water Levels

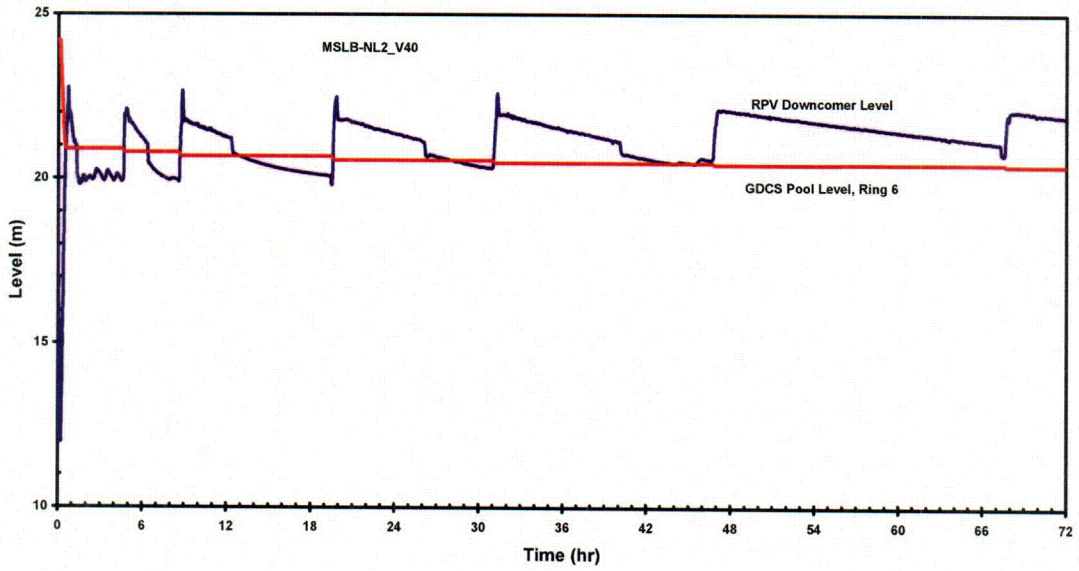

Figure 6.2-52_6 MSLB-NLW_V40 – GDCS and DC Water Levels

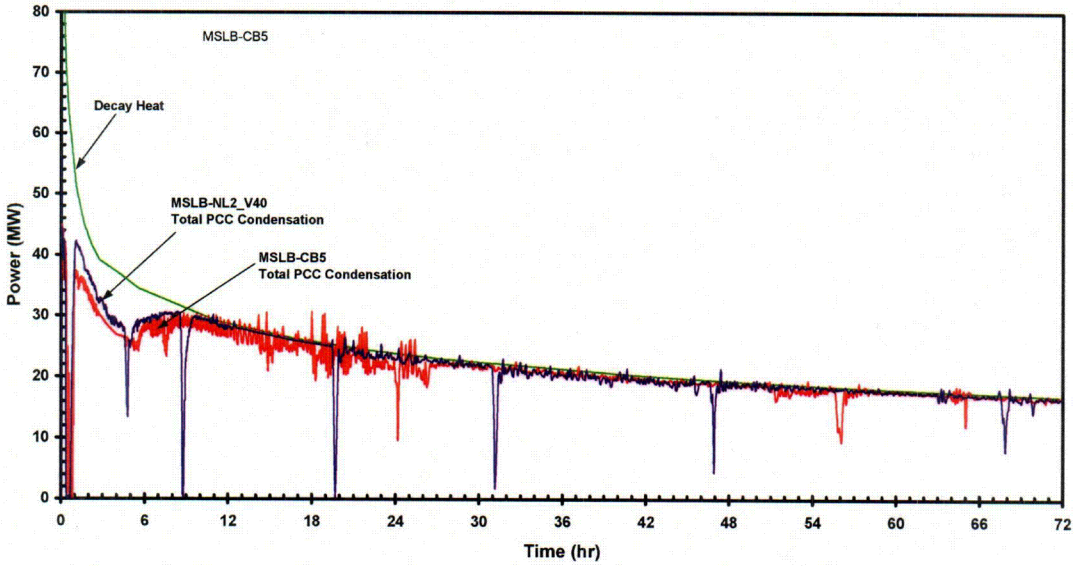

Figure 6.2-52_7 MSLB-CB5 vs. MSLB-NLW_V40 – Total PCC Condensation Powers

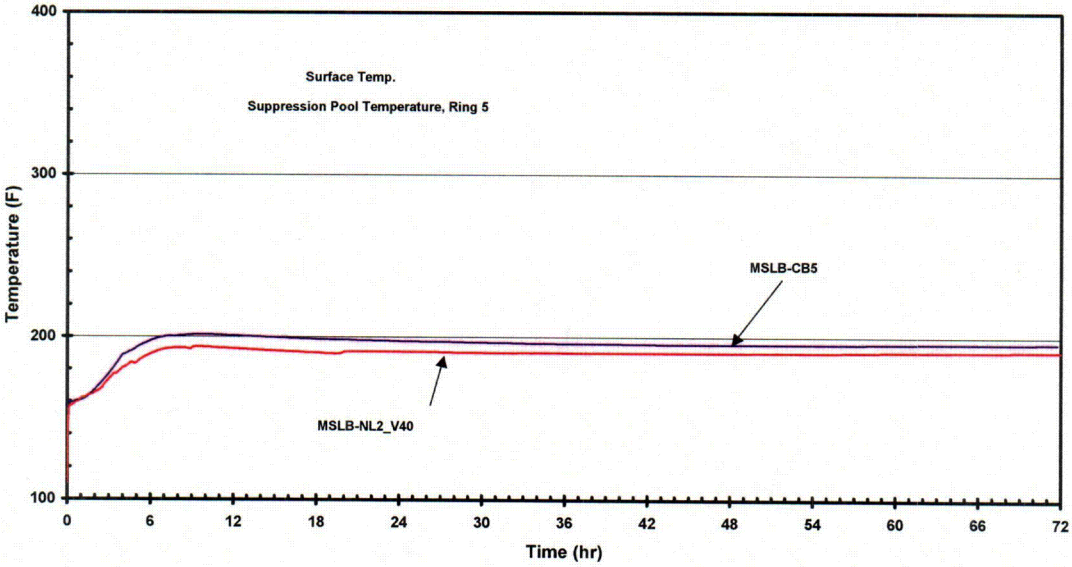

Figure 6.2-52_8 MSLB-CB5 vs. MSLB-NLW_V40 – Suppression Pool Surface Temperatures

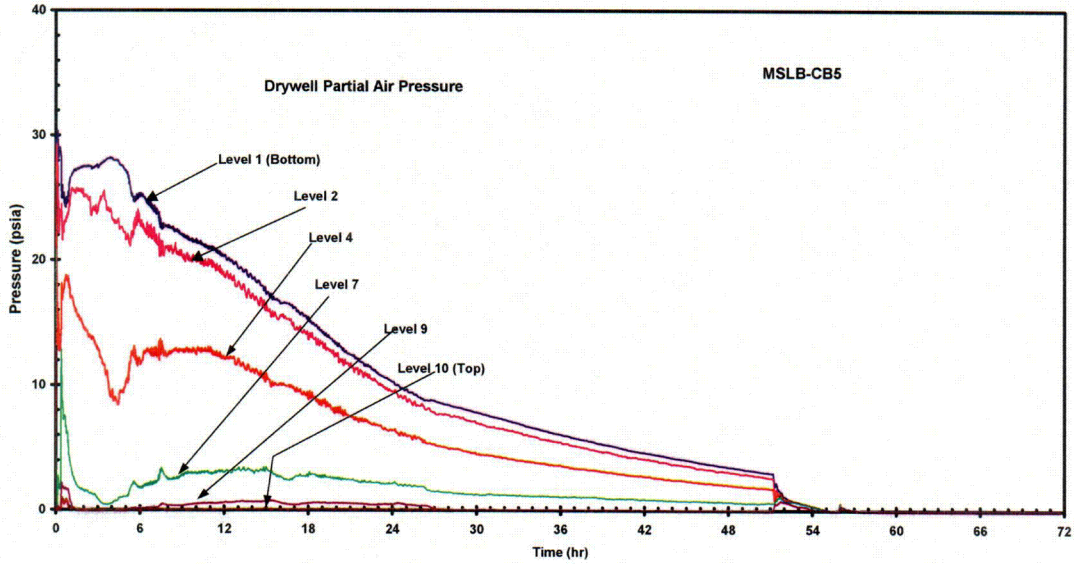

Figure 6.2-52_9 MSLB-CB5 – Drywell Partial NC Gas Pressures
(Level locations are consistent with those in Figure 6.2-53_10)

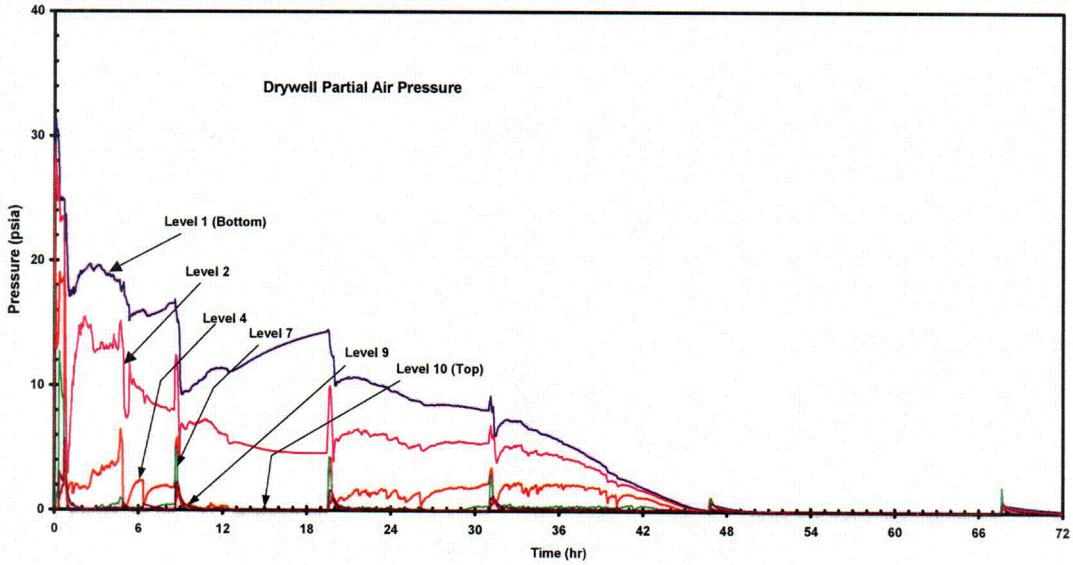

Figure 6.2-52_10 MSLB-NL2_V40 – Drywell Partial NC Gas Pressures

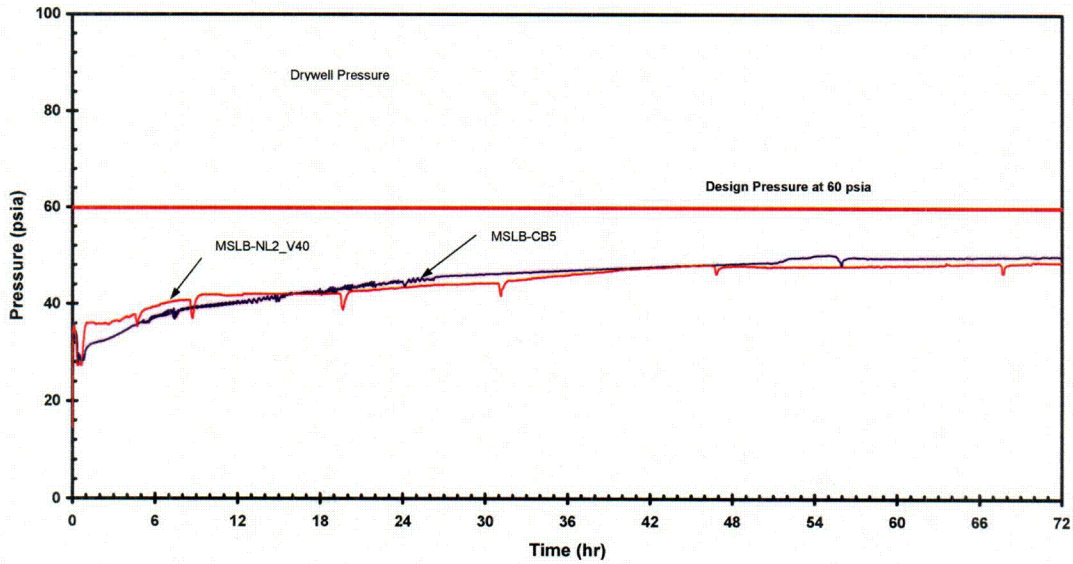

Figure 6.2-52_11 MSLB-CB5 vs. MSLB-NLW_V40 – Drywell Pressures

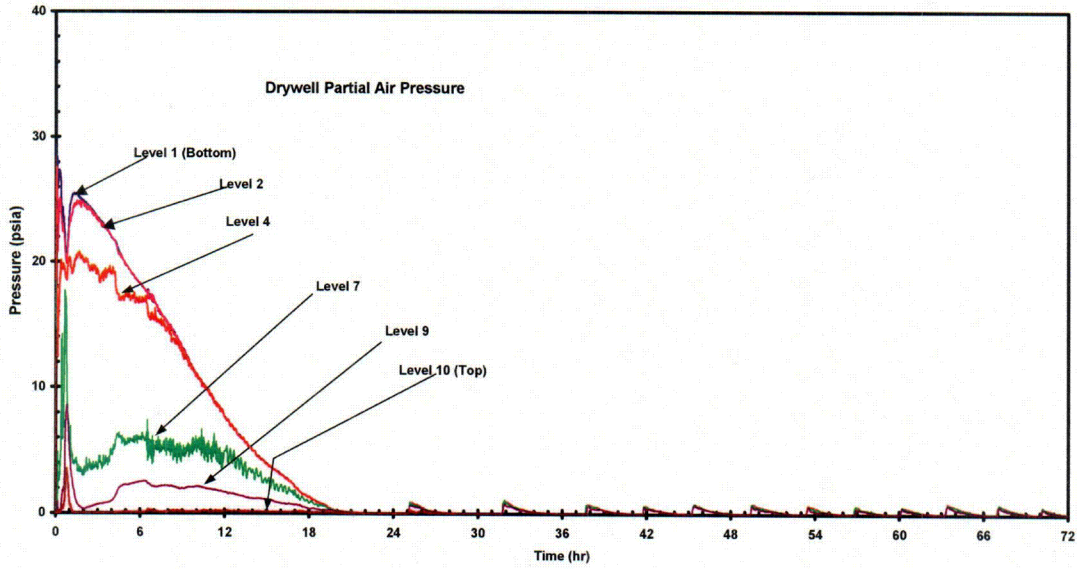

Figure 6.2-52_12 MSLB-CB6 – Drywell Partial NC Gas Pressures
(Level locations are consistent with those in Figure 6.2-53_10)

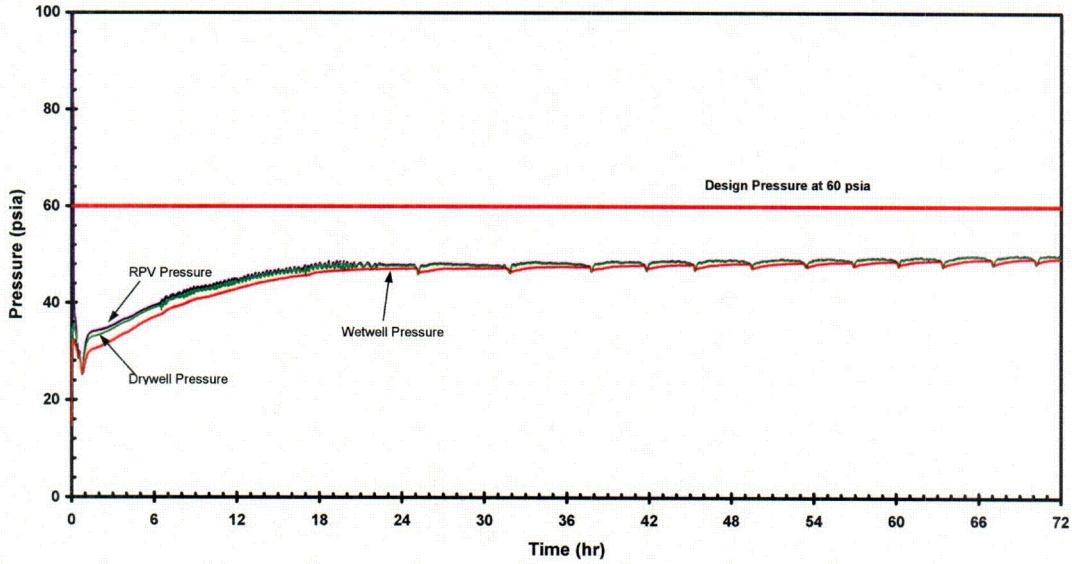

Figure 6.2-52_13 MSLB-CB6 – RPV, Drywell and Wetwell Pressures

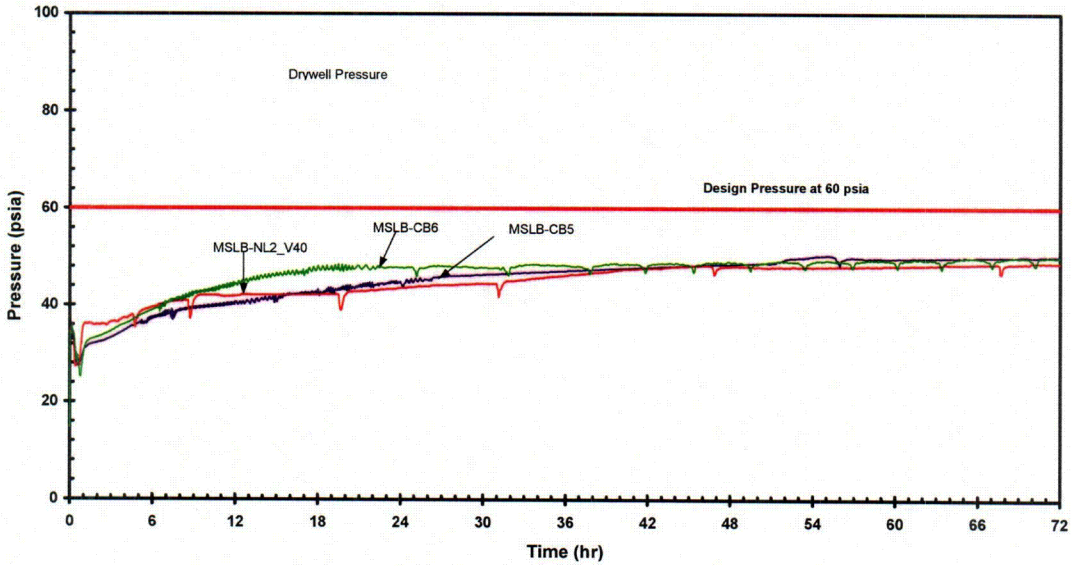

Figure 6.2-52_14 Drywell Pressure comparison – MSLB-CB6, MSLB-CB5 and MSLB-NL2_V40

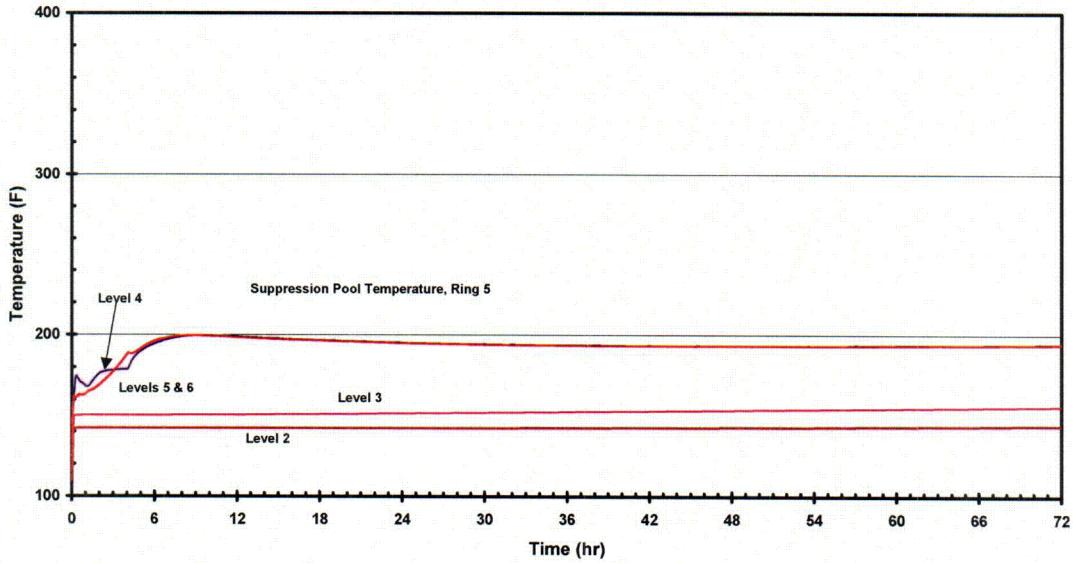

Figure 6.2-52_15 MSLB-CB6 – Suppression Pool Temperatures

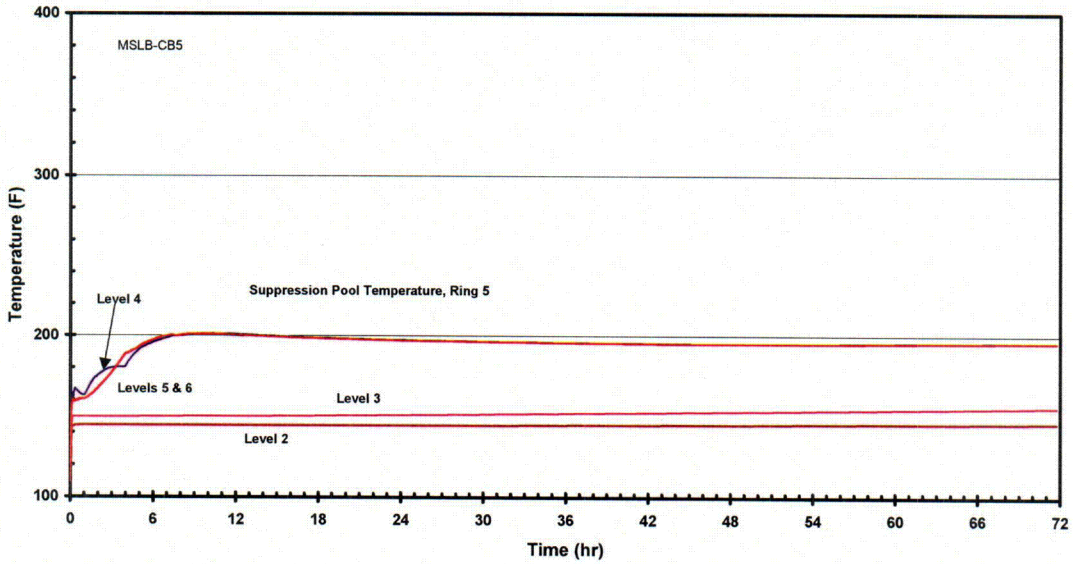

Figure 6.2-52_16 MSLB-CB5 – Suppression Pool Temperatures

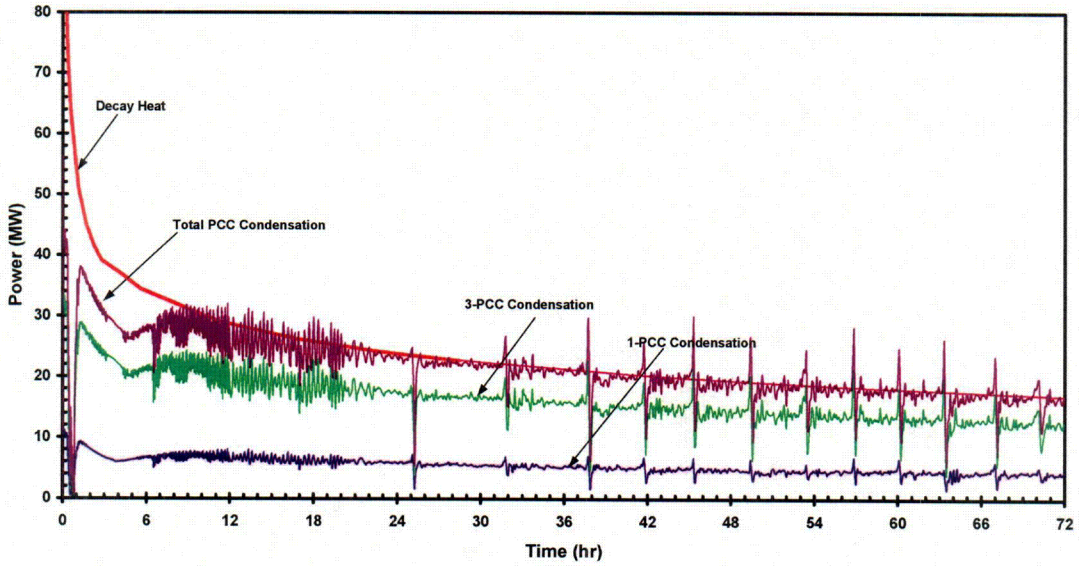

Figure 6.2-52_17 MSLB-CB6 – PCC Condensation Power

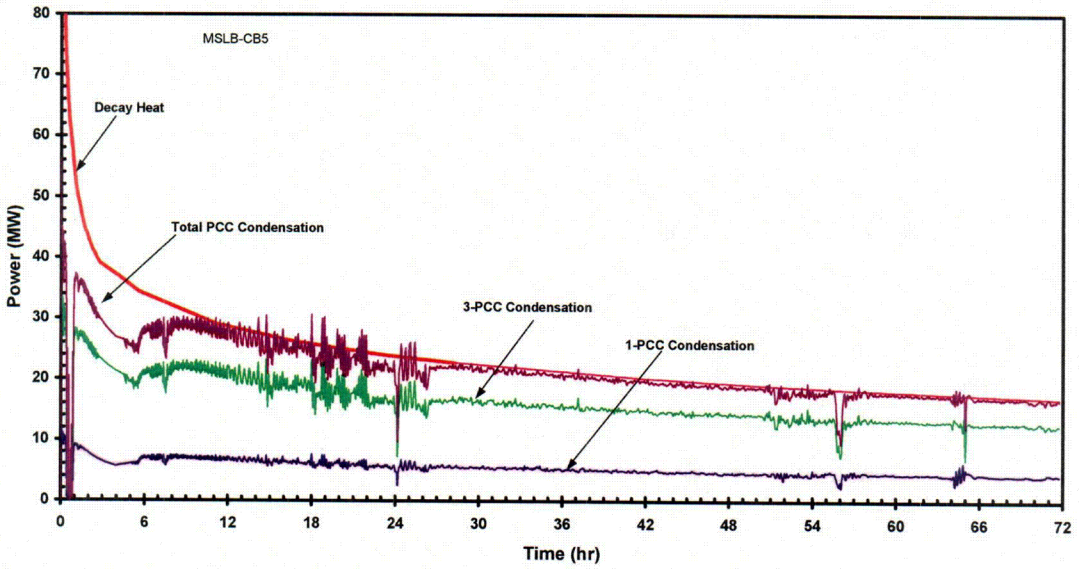

Figure 6.2-52_18 MSLB-CB5 – PCC Condensation Power

Response to RAI 6.2-52 C

The newer DCD version of the TRACG model (shown in Figures 6.2-6 to 6.2-8, DCD Tier 2, Rev. 1) was used in the evaluation of the main steam line break (MSLB) presented in the DCD Tier 2, Rev. 1. The following paragraphs discuss the containment response to the MSLB using this model, including the non-condensable (NC) gases holdup, mixing and stratification. The discussion also includes the impacts from the additional changes in the model due to the design changes and the model refinements.

These discussions will be included in the Supplement in DCD Section 6.2.

(1) DCD TRACG Model

The DCD TRACG Model is shown in Figures 6.2-52_19 and 6.2-52_20 (from Figures 6.2-6 and 6.2-7, DCD Tier 2, Rev. 1). This model is based on COMB-6 (discussed in response to RAI 6.2-52 B), incorporating the changes listed in Table 6.2-6a (DCD Tier 2, Rev. 1). The key differences in the containment between the DCD model and the COMB-6 model are:

(1) The GDCS pool and air space connect to the DW, and the PCC drain tanks in the model COMB-6 are eliminated,
(2) Separate regions to model the expansion pool and the dryer/separator storage pool,
(3) Air gap between the RPV and the reactor shield wall is modeled (Figure 6.2-52_20, Axial Levels 24 to 34, Ring 4).

Items 1 and 2 are due to the design changes, and Item 3 is due to the model refinements.

(2) Main Steam Line Break – Base Case (MSL-8F_1DPV-72)

The containment responses to a postulated main steam line break (MSLB) are discussed in the following paragraphs and figures. This case considers a single failure of 1 DPV and nominal conditions (Table 6.2-6, DCD Tier 2 Rev 1), and assumes 100% double-ended break.

Figure 6.2-52_21 shows the RPV, DW and WW pressures, and Figure 6.2-52_21a shows the same responses in short-term time scale.

Following the postulated LOCA, the drywell pressure increased rapidly leading to the clearing of the PCC and main vents. At around 5 seconds, the DW pressure reaches a peak value of 248.7 kPa (36.1 psia). This peak pressure is below the design pressure of 413.7 kPa (60 psia) with large margin. During this blowdown period, significant amount of non-condensable (NC) gases is purged into the WW and pressurizes the WW. At around 0.12 hrs, the RPV pressure drops below the pressure point at which the GDCS water is allowed to inject into the downcomer by gravity head. The subcooled GDCS water continues flowing into the vessel, reduces the steaming from the RPV and the DW pressure. At around 0.31 hrs, the DW pressure drops below the WW pressure, causing the openings of vacuum breakers and allowing some NC gases to flow back into the DW. Consequently, the system pressures drop to a value of about 185 kPa.

Subsequently, the decay heat overcomes the subcooling of the GDCS water and steaming resumes (at ~ 0.45 hrs, Figure 6.2-52_21a). The resumption of RPV steaming causes the drywell pressure to increase again starting from 0.45 hrs.

Figure 6.2-52_22 shows the downcomer collapsed level, Figure 6.2-52_23 shows the GDCS pool water levels. After the initiation of the GDCS flow, the GDCS pool water level drops and consequently the downcomer collapsed level rises. For the rest of the transient, the downcomer collapsed level maintains an equilibrium position at around the elevation of the DPVs (Stub Tube elevation at 21.91 m). The corresponding GDCS pool equilibrium level is about 21.4 m.

Figure 6.2-52_24 compares the total heat removal by the PCCs with the decay heat. From 6 to 30 hrs, about 90 to 95% of the decay heat is removed by the PCCS and discharged to the PCC pools, which are outside of the containment. The residue decay heat (about 5 to 10% not removed by the PCCS) corresponds to the reduction in RPV steaming rate. The reduction is due to that a small portion of the decay heat is used to heat up the incoming cooler GDCS water. Figure 6.2-52_25 compares the GDCS pool water temperature with the downcomer water temperatures. In this design, the hot PCCS condensate (~105 °C) drains to the GDCS pool and mixes with the remaining water (for MSLB case, ~ 1000 m^3) in the pools. The GDCS water injected into the RPV during the MSLB transient is at a temperature considerable lower than that for the PCC condensate. For the reference design used in the Report NEDC-33083P-A, "TRACG Application for ESBWR", the hot PCCS condensate drains directly into the RPV. After 60 hrs, the mixture temperature approaches an equilibrium temperature of 95 °C (Figure 6.2-52_25). Subsection (4) discusses the effect of reduced steaming rate and NC gases circulation pattern.

Figure 6.2-52_26 shows the PCC pool water level. The PCC pool water level drops due to boiloff by the decay heat. At 39 hrs, the pool level drops below the elevation of 29.6 m, (or top ¼ portion of the PCC tube length uncovered). The connection valves open to allow the water from the Dryer/Separator storage pools to flow into the PCC pools. This increase in PCC tube coverage causes a small increase in PCC condensation power (Figure 6.2-52_24).

Figures 6.2-52_27 through _31 show the NC gases pressures in the DW annulus, lower DW, air gap between the RPV and the reactor shield wall, the DW head airspace, and the GDCS pool airspace. Most of the initial NC gases in the DW annulus are purged into the WW within 3 hrs. Small amount of NC gases remain in the DW regions for the rest of the transient. It takes about 72 hrs to purge most of the NC gases in the DW head airspace (Figure 6.2-52_30). About 60% of the NC gases that back filled the airspaces created by the draining of the GDCS pool water remain in the GDCS pool airspace (Figure 6.2-52_31).

Figures 6.2-52_32 and _33 show the suppression pool water temperatures at different elevations in Ring 7 (next to the horizontal vents) and Ring 8 (away from the horizontal

vents). Shortly after the blowdown period, the suppression pool stratification model prevents any mixing in the bottom three levels (Levels 25, 26 and 27) in the suppression pool. (The stratification model zero's the flow areas in the radial direction at these 3 levels, when there is no discharge from the vent, or SRV discharge line to the lower level). Figure 6.2-52_33 shows that the water temperatures in these levels (in Ring 8) remain constant for the 72 hrs transient after the initial heatup from the blowdown. After the blowdown, the pool surface temperatures (Level 29 in Rings 7 and 8) increase an additional 6 °K as the results of the energy/steam in the PCC vent flow and the increase in the WW air temperatures (Figures 6.2-52_34 and 6.2-52_35).

Figures 6.2-52_34 and _35 show the wetwell gas temperatures at different elevations in Ring 7 (next to the vacuum breakers and leakage) and Ring 8 (away from the vacuum breakers). Air temperatures at Levels 29 and 30 follow closely with pool surface water temperatures. The increase for the gas temperature at the top WW corner next to the leakage hole (Level 31, Ring 7) is larger than others due to the inflow of hotter gas from the DW via the leakage hole and the gas stratification model. The WW gas stratification model applies a large value of loss coefficient (100000) at the axial faces (Rings 7 and 8 in Level 30) and restricts the mixing between the cells at Levels 30 and 31.

(3) Comparison between the DCD Base Case and the Application Report Case

Comparing to the results from the Case MSLB-CB6 (Response to RAI 6.2-52b), there are three major points that are different in responses.

(1) In the Case MSLB-CB6, all the initial NC gases in the DW are purged into the WW in 21 hrs (Figure 6.2-52_12). After that time, a small amount of NC gases return to the DW during each vacuum breaker opening but are purged back to the WW in 2~3 hrs by the PCCS. In the Base Case MSL-8F_1DPV-72, most of the initial NC gases in the DW are purged into the WW in 3 hrs.
(2) In the Case MSLB-CB6, the total PCC condensation power follows closely with the decay heat (after 9.5 hr) (Figure 6.2-52_17). In the Base Case MSL-8F_1DPV-72, about 5 to 10% of the decay energy is not removed by the PCC and heats up the remaining water in the GDCS pool. Since portion of the decay energy is used to heat up the imcoming cooler GDCS water, the total RPV steaming rate is reduced in the Base Case MSL-8F_1DPV-72.
(3) In the Case MSLB-CB6, the DW pressure reaches the long-term peak value after 21 hrs (Figure 6.2-52_13). In the Base Case MSL-8F_1DPV-72, the DW pressure increases continuously and reaches the peak value at 72 hrs, due to the heatup of the remaining water in the GDCS pool, the heatup of WW gas at the ceiling level, and the continued purging of air from the air spaces in the DW head and the GDCS pools into the WW.

Two parametric cases are performed to provide additional explanations on these differences. The following paragraphs discuss the results of these cases and address the differences.

(4) Effect of GDCS Pool Location (connecting to DW versus to WW)
One of the major nodalization differences between the DCD model and the Application Report model is the GDCS pool location, connecting to the DW versus to the WW. To demonstrate the impact of this change, a parametric Case MSL-8F_1DPVGD2-72 is performed. This case is modified from the Base Case MSL-8F_1DPV-72. This case artificially reduces the GDCS pool volumes in the bottom layer (Level 33, Figure 6.2-52_20) by 90%, and the volumes in the upper layer by 10%. This change is to reduce the amount of remaining water in the GDCS pools after the levels between the RPV and GDCS pools have reached the equilibrium position.

Key results from this parametric case are shown in Figures 6.2-52_36 to _39. Compared to the base case (Figure 6.2-52_25), the GDCS pool water temperature (Figure 6.2-52_38) increases to a higher long-term value in a shorter time period. In this parametric case, the total PCC condensation power (Figure 6.2-52_37) follows closer with the decay heat (closer than that in the base case) during the transient.

Figure 6.2-52_39 shows the NC gas pressures. The NC gases in the upper half of the DW annulus are purged into the WW in the first 6 hrs while the NC gases in the lower half remain in the DW. At 15 hrs, some of the NC gases in the lower half move to the upper half as the result of change in DW gas circulation pattern. These NC gases remain in the DW for the rest of the transient, while it takes 3 hrs to purge most NC gases from the DW to the WW for the base case (Figure 6.2-52_27).

The difference in purging time and NC gases distribution between the base case and the parametric case can be attributed to the difference in the DW gas circulation patterns. Figures 6.2-52_40 and 6.2-52_41 show the total PCC steam inlet flows for the base case and the parametric case. During the first 6 hrs, the total PCC steam inlet flow for the base case is about 10% less than that in the parametric case. This difference in steam flow in the DW causes the difference in the DW gas circulation patterns. Figures 6.2-52_42 and 6.2-52_43 show the gas velocities (in the vertical direction) during the first 6 hrs at Levels 25 and 29, Rings 5 and 6 in the DW Annulus. The NC gas circulation stops at about 4 hrs for the parametric case, while it goes on for more than 6 hrs for the base case. This gas circulation helps purging the NC gases in the lower portion of the DW annulus to the WW.

(5) Effect of Break Location
The gas circulation pattern affects the timing of the initial removal and the subsequent removals of the NC gases returning to the DW due to vacuum breaker openings. The circulation pattern depends on several parameters, such as the DW annulus geometry, the strength and location of the steam source. To cap the impact of the NC gas distribution on the DW pressure, a parametric Case MSL-8F_1DPVL23-72 is performed. The input in this case is modified from the Base Case MSL-8F_1DPV-72. This case artificially lowers the MSLB break elevation (connection to the DW annulus) from 22.82 m to the lower DW (Level 23, Cell 1, in Figure 6.2-52_20). This change is to have the steam

source at the lowest possible point in the DW to force all NC gases in the DW annulus into the WW.

Key results from this parametric case are shown in Figures 6.2-52_44 to _48. The DW pressure increases continuously and reaches the peak value at 72 hrs. The peak DW pressure is 314.6 kPa. The total heat removal by the PCCs (Figure 6.2-52_45) is similar to that for the base case. Due to the lowest location for the steam source, all the initial NC gases in the DW annulus are purged into the WW in 2 hrs. For the same reason, the purging of the NC gases in the DW head and GDCS pool airspaces is slightly less effective as compared to the base case (Figures 6.2-52_47 and _48 versus Figures 6.2-52_30 and _31). As a result, the DW pressure for the base case is higher than that for the parametric case. Figure 6.2-52_49 shows the comparison of the DW pressures between the base case and the parametric case. It should be noted that the margin to the design pressure is greater than 29% for the base case, at the end of the 72 hrs transient.

(6) Summary

Subsection (1) describes the differences in TRACG models between the DCD analyses and that in the Application Report. Subsection (2) discusses the containment responses to the MSLB using the DCD TRACG model, including the NC gases holdup, mixing and stratification. Subsection (3) discusses the differences in response due to the changes in the nodalization. Two parametric cases are performed to provide additional explanations on these differences. These parametric cases are discussed in Subsections (4) and (5).

One of the major nodalization differences between the DCD model and the Application Report model is the GDCS pool location, connecting to the DW versus to the WW. For the DCD MSLB, significant amount of water remains in the GDCS pools after the levels between the RPV and GDCS pools have reached an equilibrium position. The hot PCCS condensate drains to the GDCS pools and mixes with and heats up the remaining GDCS water. This heat up process accounts for 5 to 10% of the decay energy during the initial period of the transient. The total core decay energy is removed by the PCCS after the GDCS mixture temperature has reached an equilibrium temperature.

Another effect of the GDCS pool location is that the airspaces are created after the draining of the GDCS pool water. NC gases back fill these airspaces and are trapped inside these confined volumes. Purging the NC gases in these GDCS pool airspaces and that in the DW head airspace is relatively more difficult due to limited flow passages.

The other major difference in containment responses between the DCD model and the Application Report model is the gas circulation pattern. Many parameters affect the gas circulation pattern, which in turn affect the NC gas distribution and the containment pressure. Results of parametric case demonstrate that the impact of NC gas distribution on the long-term pressure can be assessed by artificially lowering the break elevation in the lowest possible elevation in the DW annulus. Figure 6.2-52_49 shows the comparison of the DW pressures between the base case and the parametric case. It should be noted that the margin to the design pressure is greater than 29% for the base case, at the end of the 72 hrs transient.

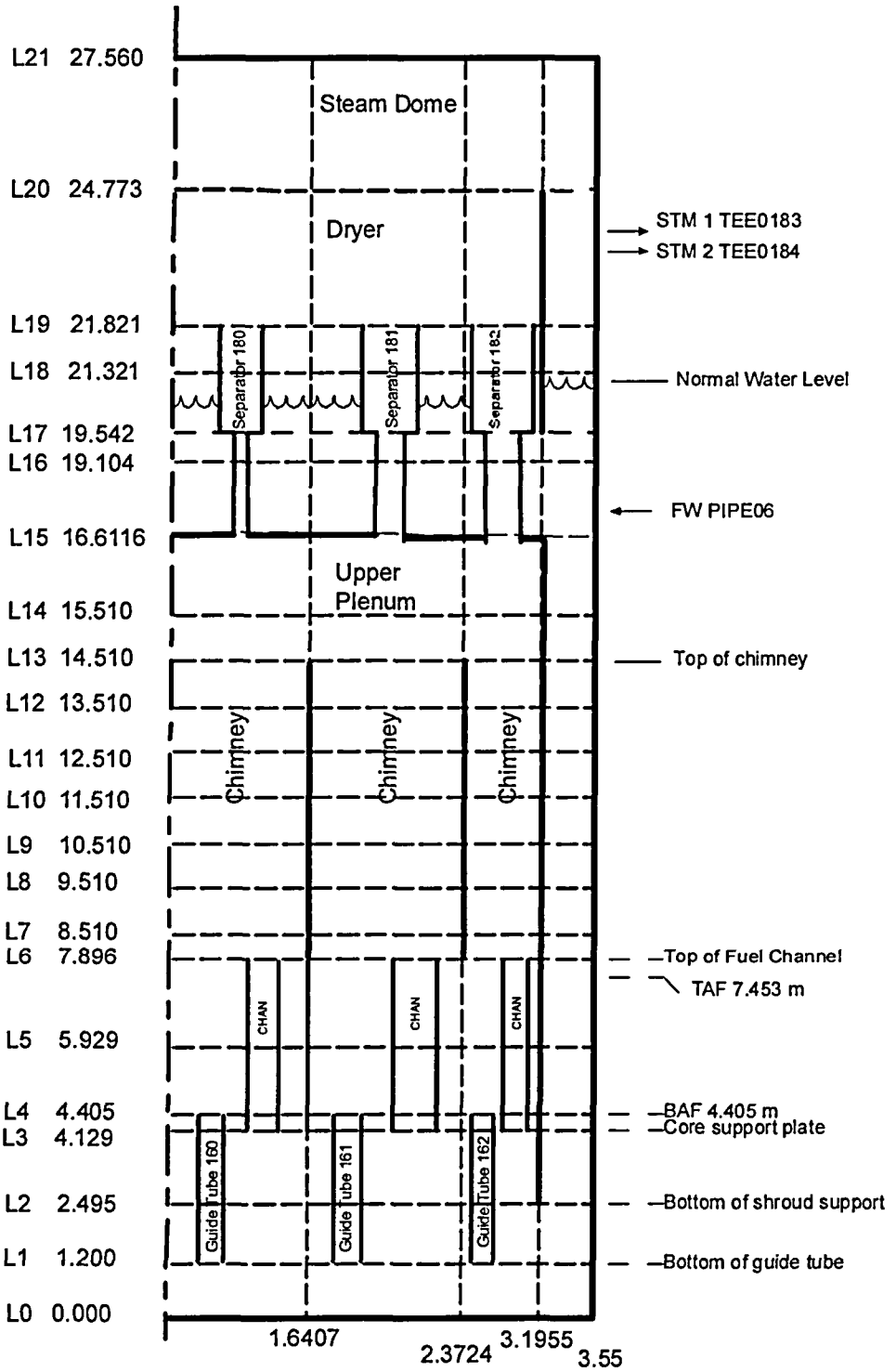

Figure 6.2-52_19 DCD TRACG Nodalization of the ESBWR RPV

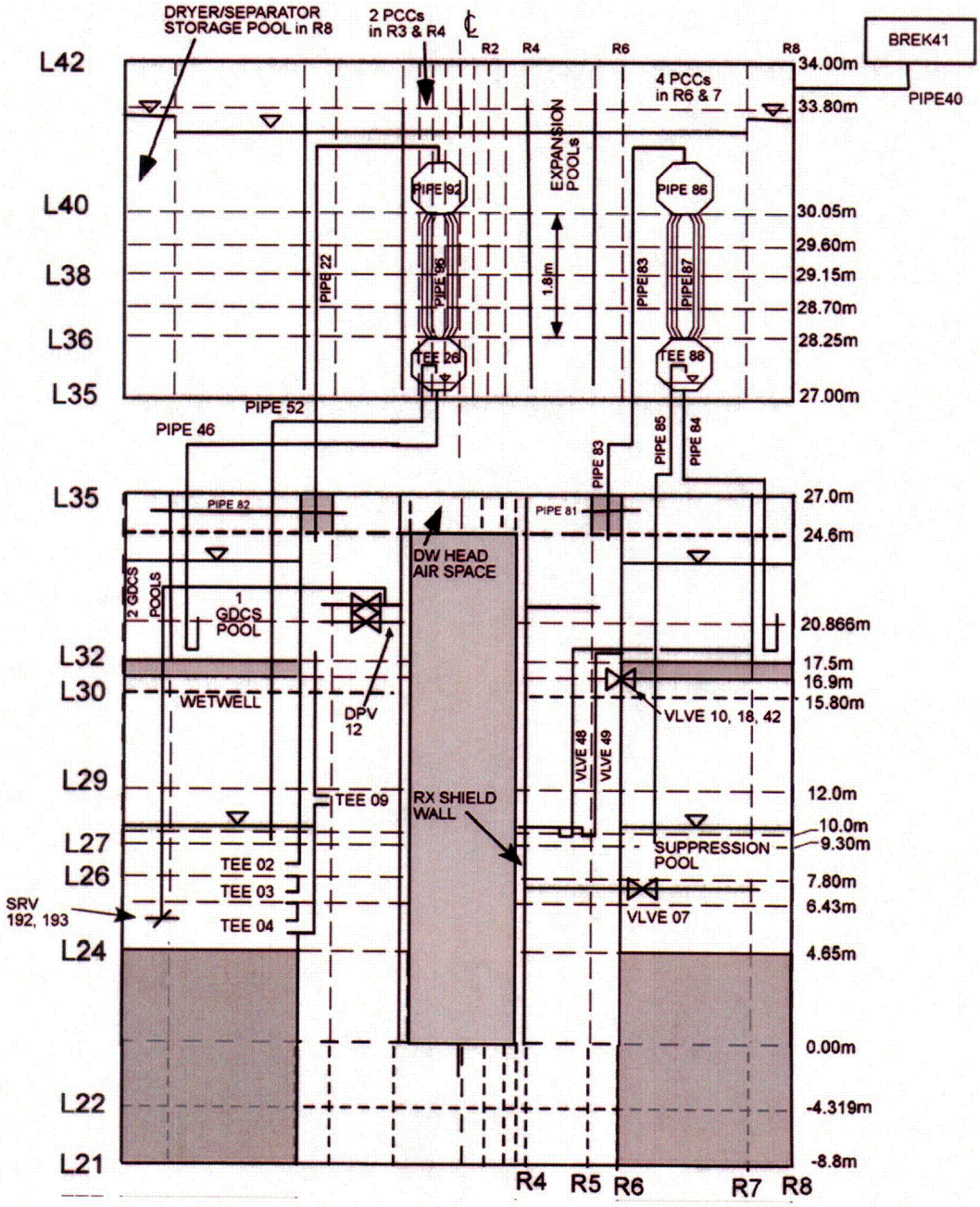

Figure 6.2-52 20 DCD TRACG Nodalization of the ESBWR Containment

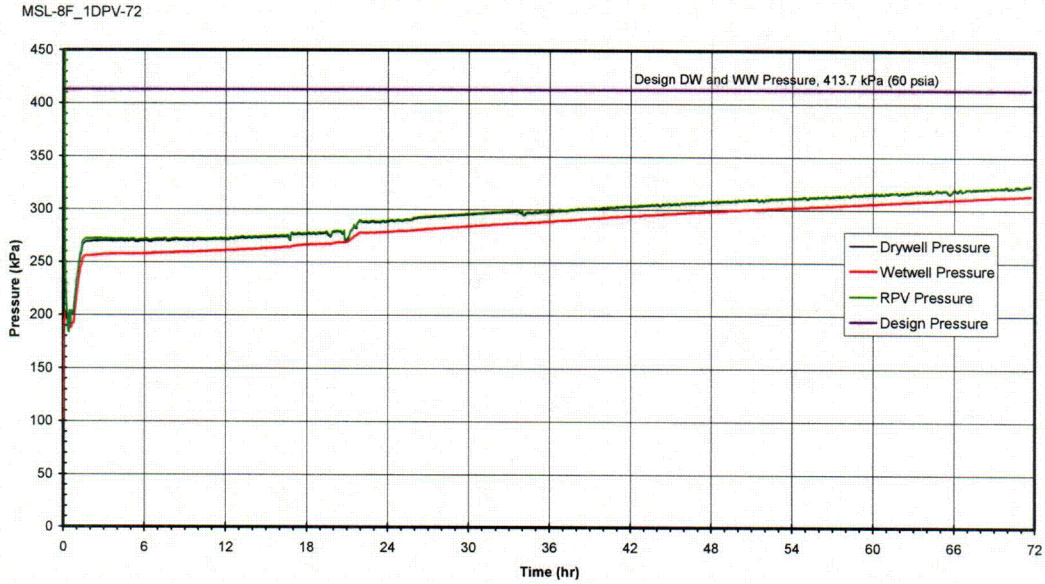

Figure 6.2-52 21 Containment Pressure Response
(Base Case: MSL-8F 1DPV-72)

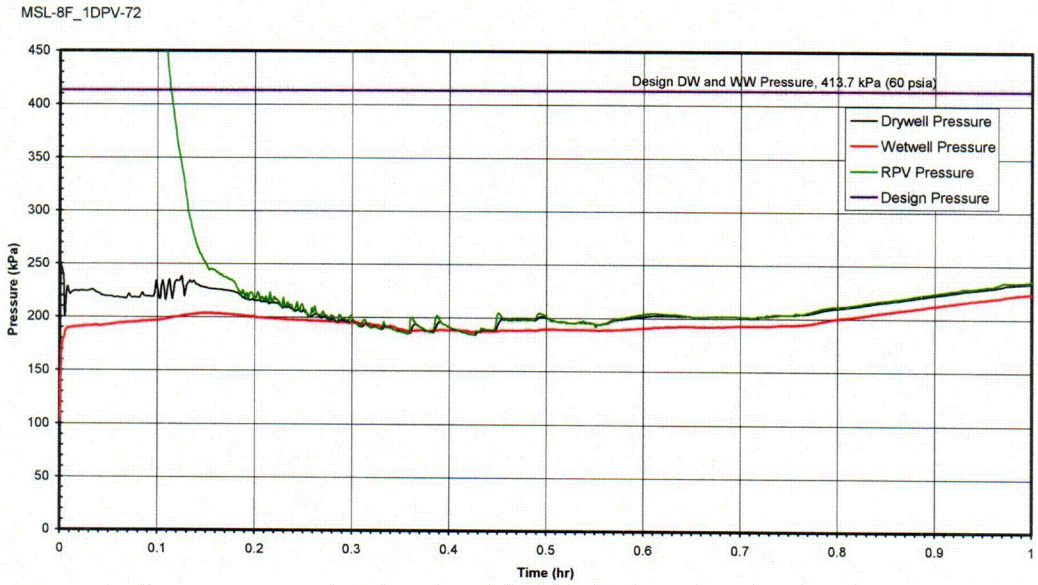

Figure 6.2-52 21a Containment Pressure Response (Short-term time scale)
(Base Case: MSL-8F_1DPV-72)

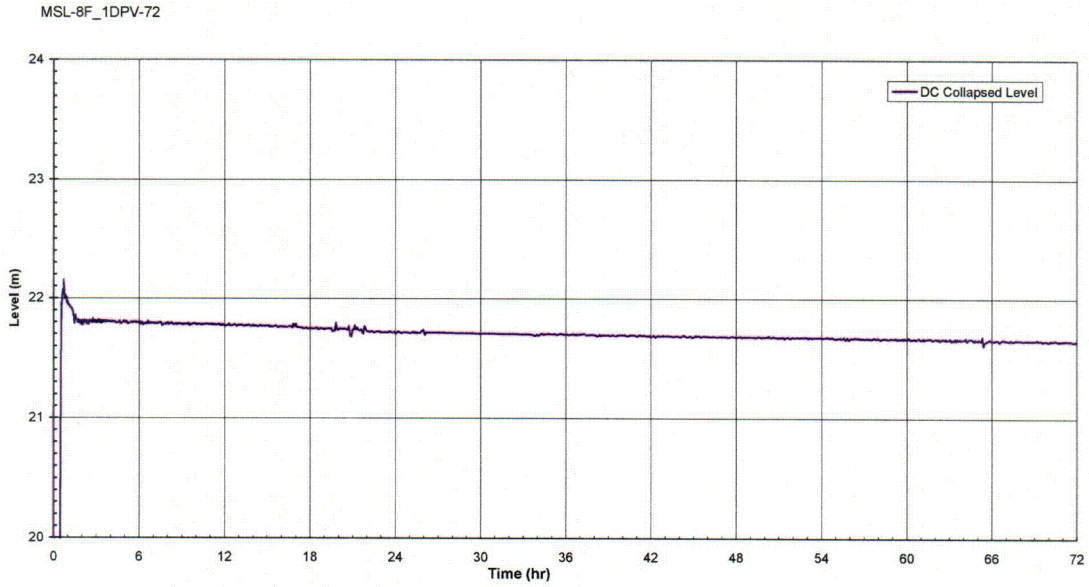

Figure 6.2-52 22 Downcomer Collapsed Level
(Base Case: MSL-8F_1DPV-72)

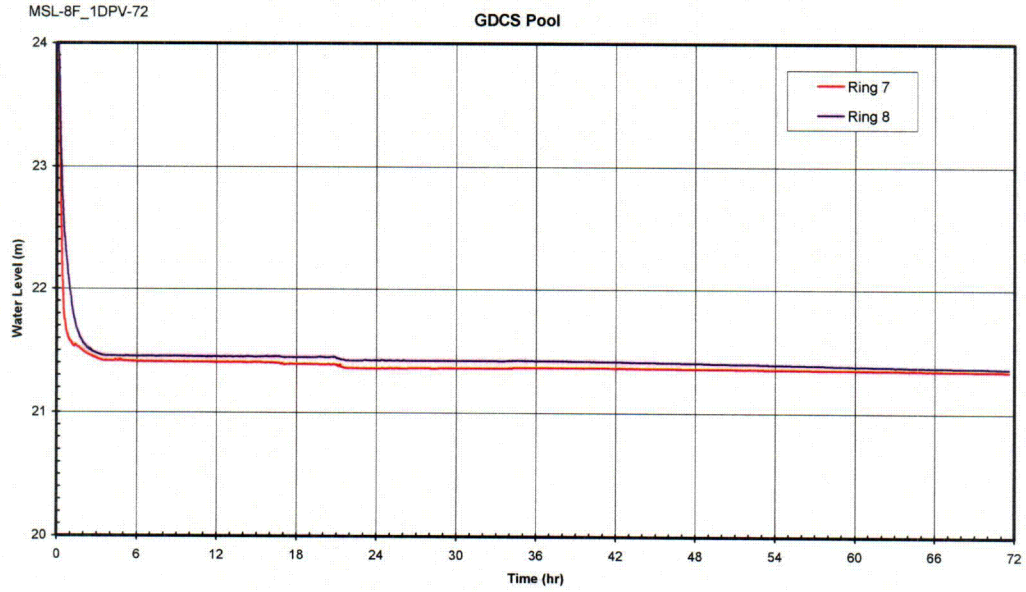

Figure 6.2-52 23 GDCS Pool Levels
(Base Case: MSL-8F_1DPV-72)

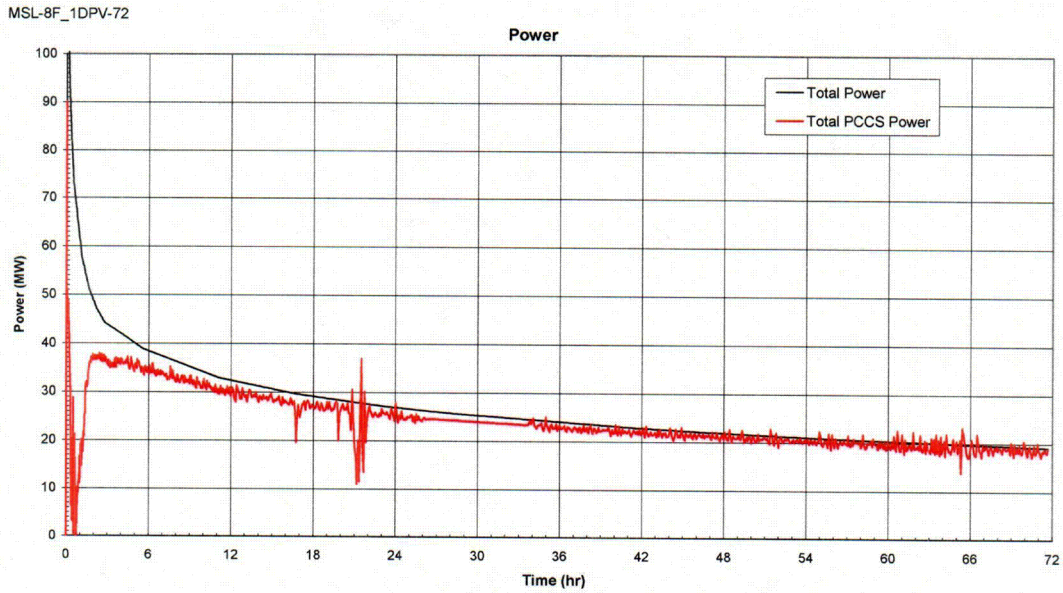

Figure 6.2-52_24 PCCS Heat Removal versus Decay Heat
(Base Case: MSL-8F_1DPV-72)

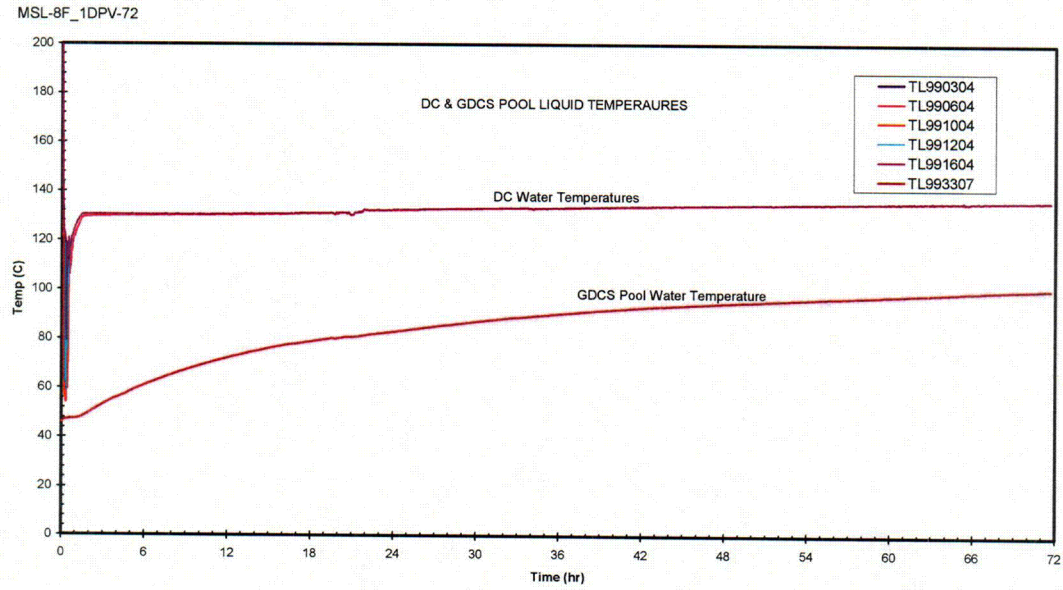

Figure 6.2-52_25 GDCS Pool Water Temperature
(Base Case: MSL-8F_1DPV-72)

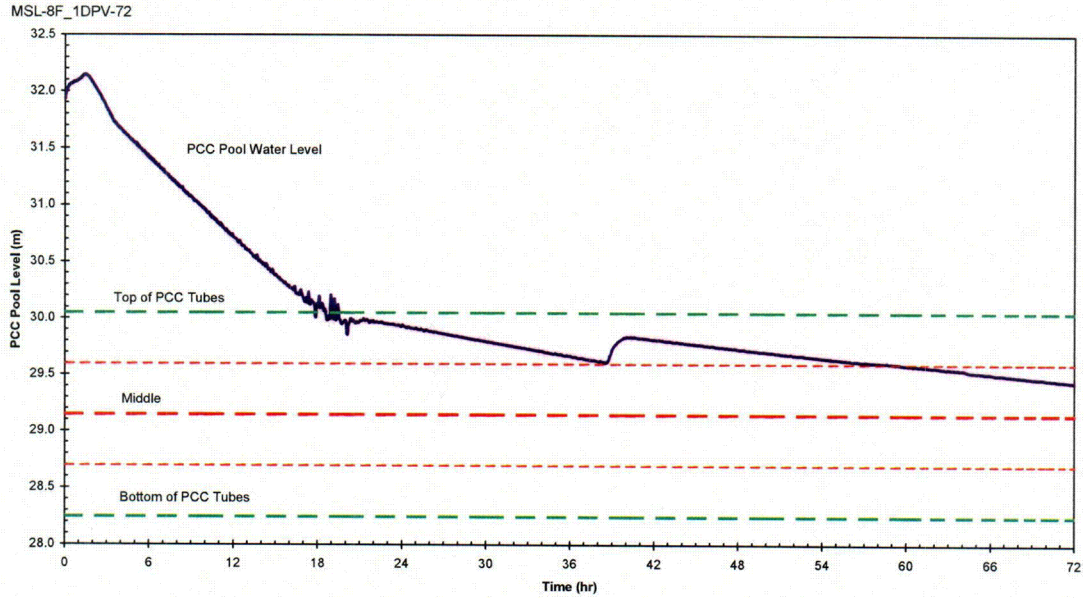

Figure 6.2-52_26 PCC Pool Water Level

(Base Case: MSL-8F_1DPV-72)

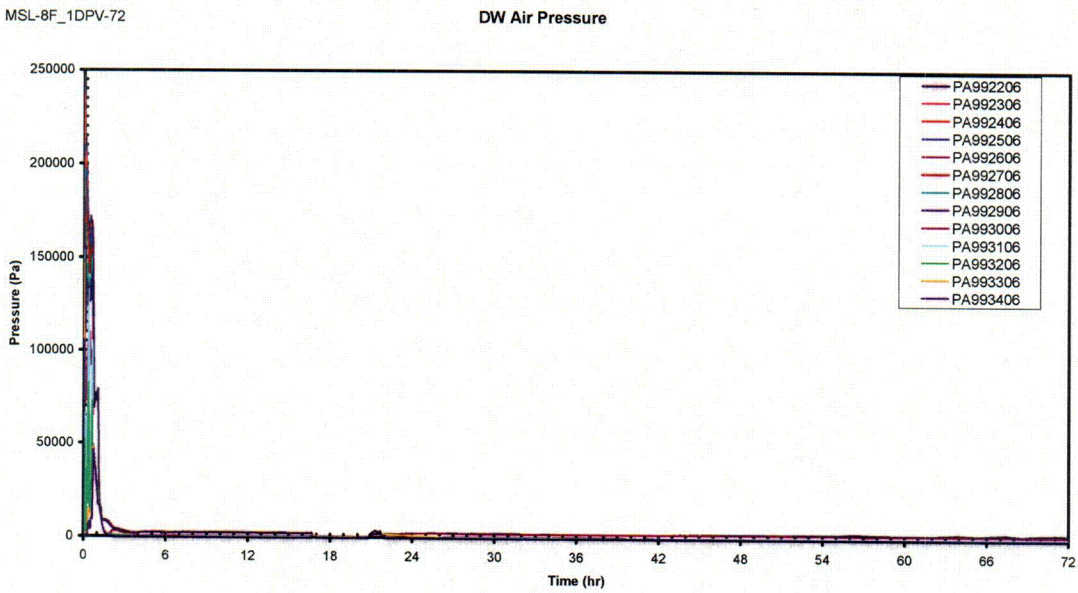

Figure 6.2-52_27 DW Annulus NC Gas Pressures (Level 23=2nd Level from Bottom, 34=Top)

(Base Case: MSL-8F_1DPV-72)

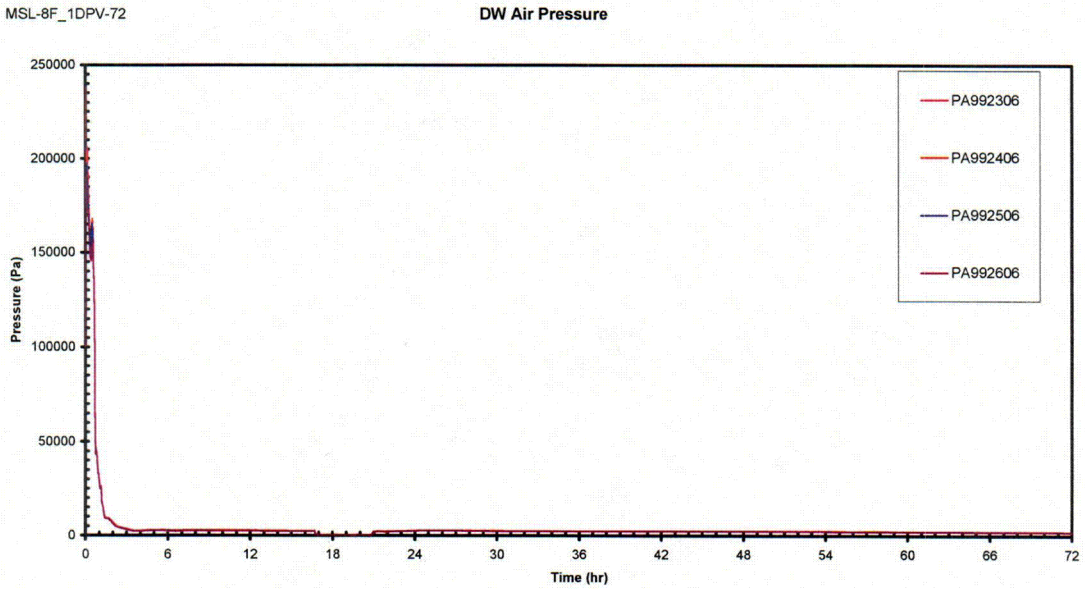

Figure 6.2-52_28 Lower DW NC Gas Pressures (23=2nd level from DW Bottom)

(Base Case: MSL-8F_1DPV-72)

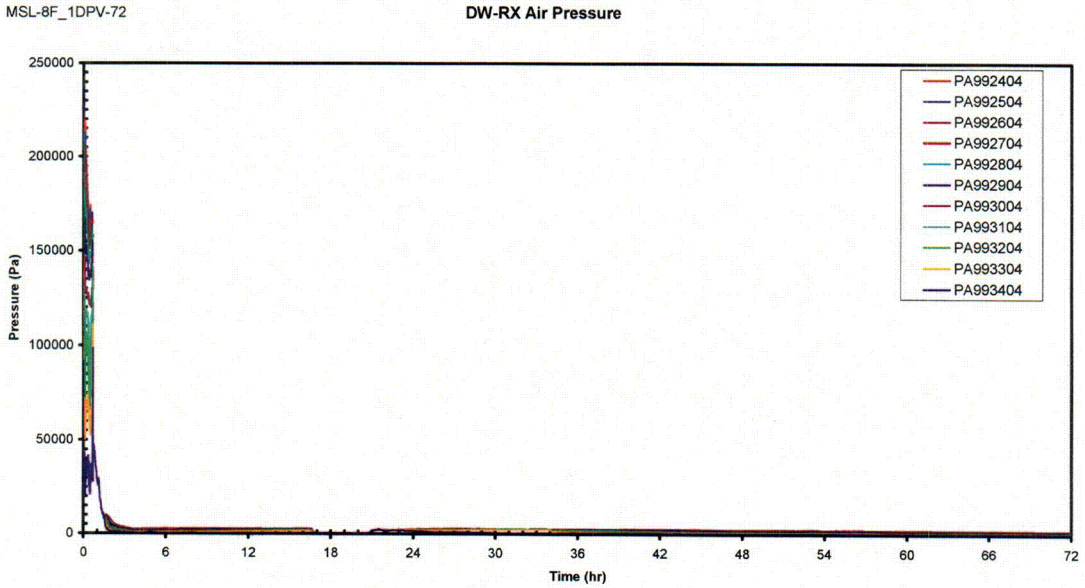

Figure 6.2-52_29 DW-Reactor Shield Wall NC Gas Pressures (Level 24=Bottom, 34=Top)

(Base Case: MSL-8F_1DPV-72)

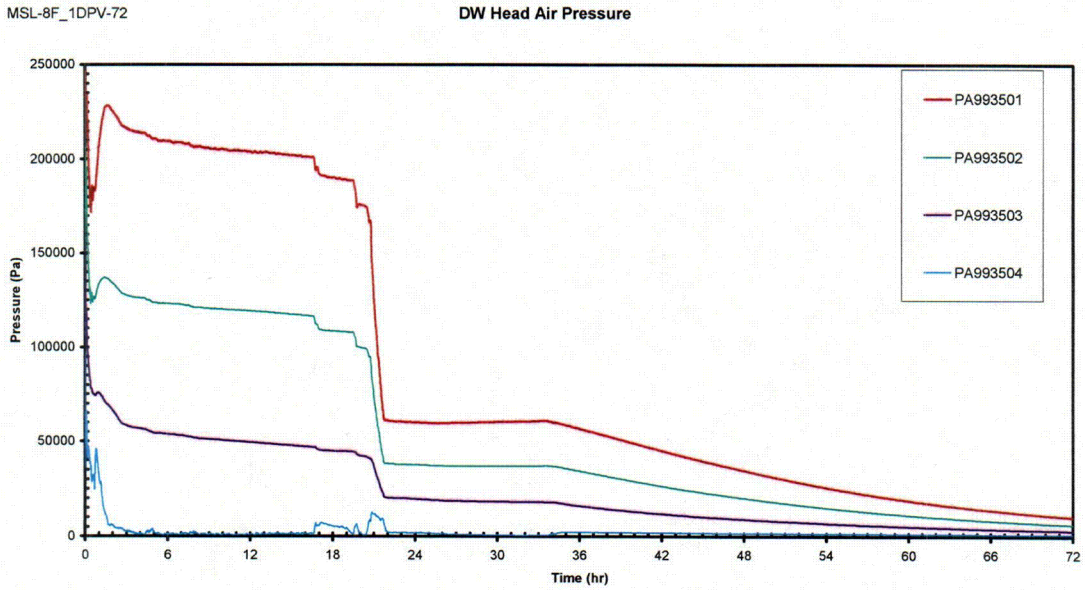

Figure 6.2-52_30 DW Head NC Gas Pressures (Level 35=Drywell Head)
(Base Case: MSL-8F_1DPV-72)

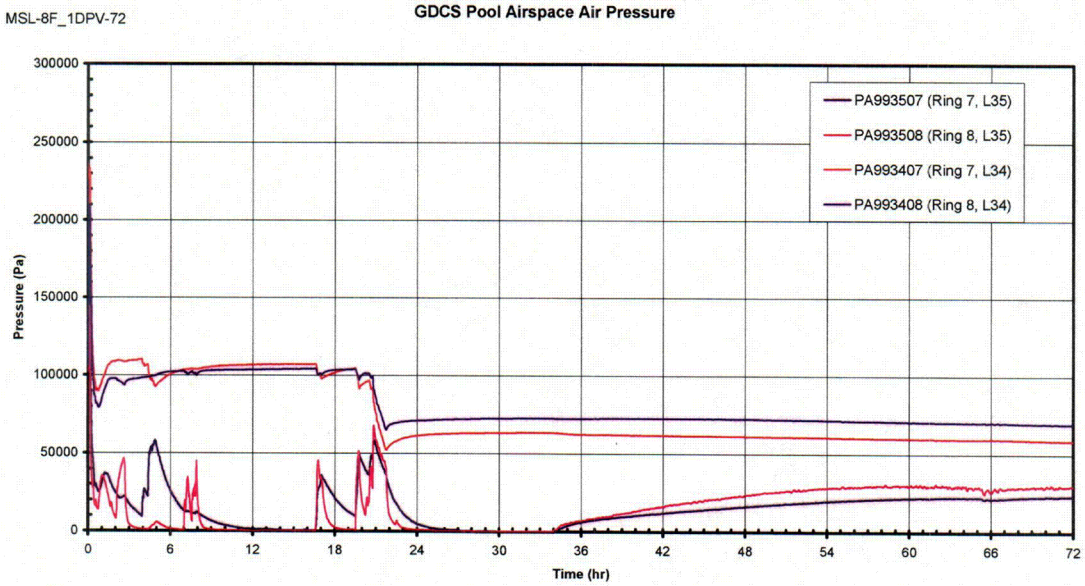

Figure 6.2-52_31 GDCS Pool Airspace NC Gas Pressures
(Base Case: MSL-8F_1DPV-72)

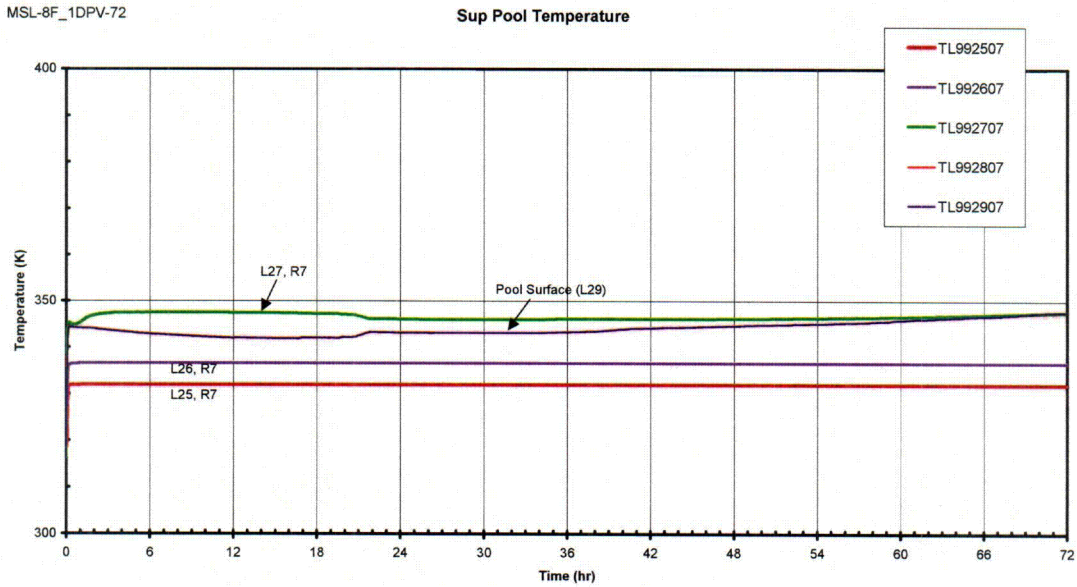

Figure 6.2-52_32 Suppression Pool Water Temperatures (at Ring 7)
(Base Case: MSL-8F_1DPV-72)

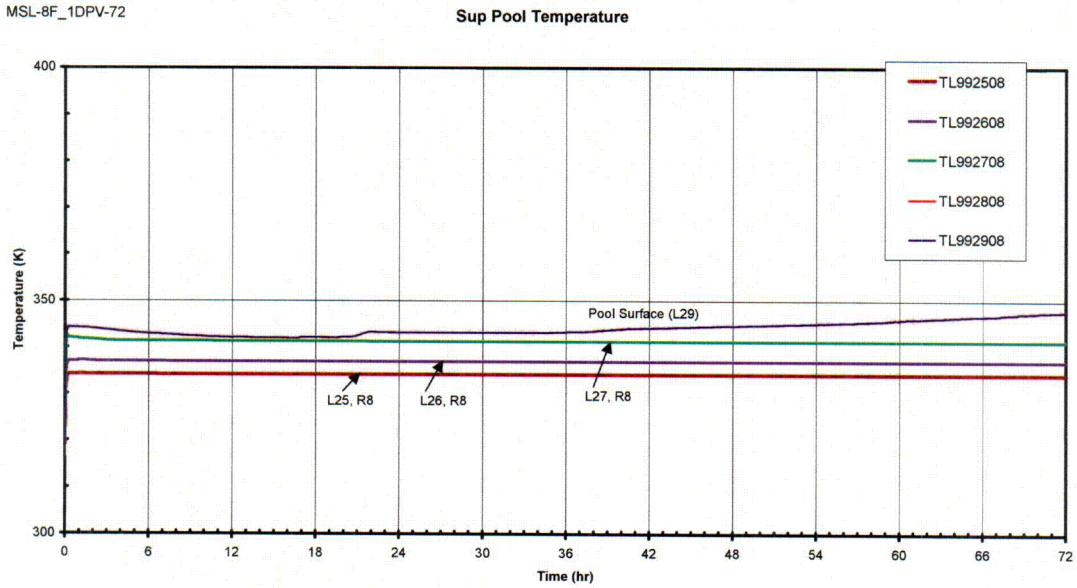

Figure 6.2-52_33 Suppression Pool Water Temperatures (at Ring 8)
(Base Case: MSL-8F_1DPV-72)

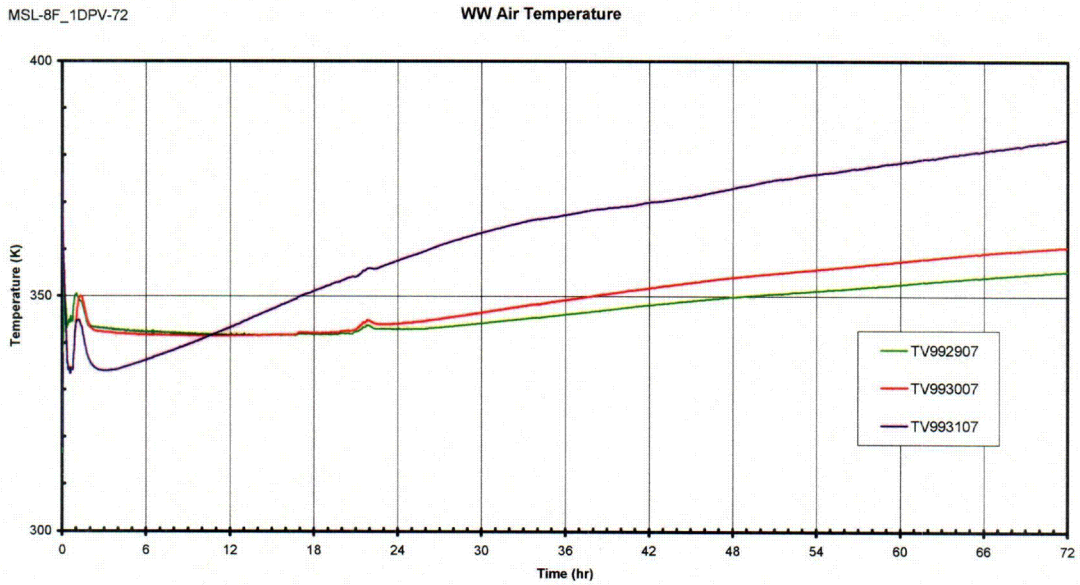

Figure 6.2-52_34 Wetwell Air Temperatures (at Ring 7)
(Base Case: MSL-8F_1DPV-72)

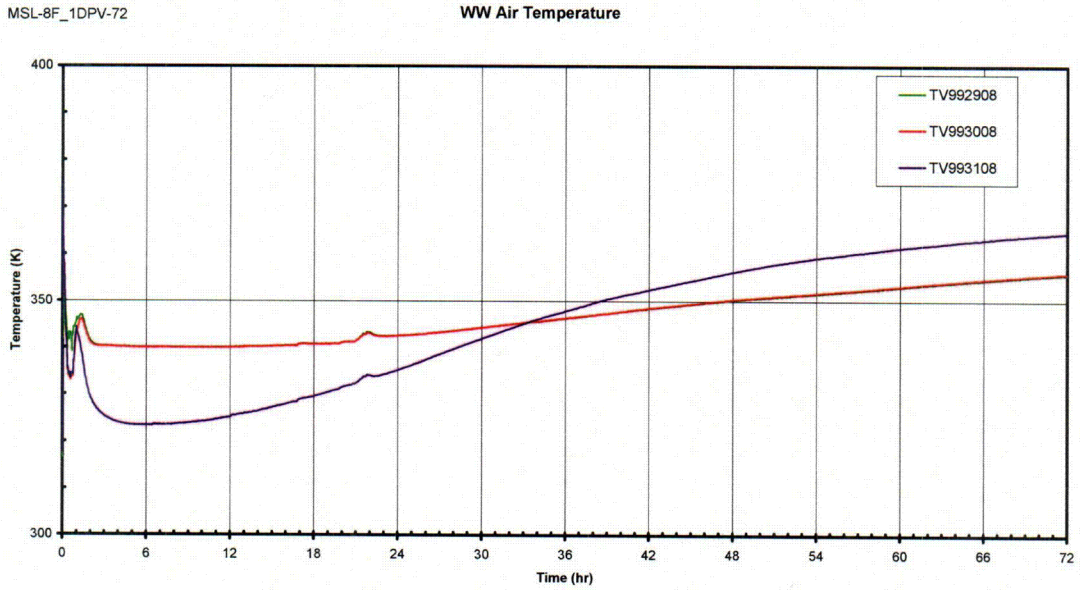

Figure 6.2-52_35 Wetwell Air Temperatures (at Ring 8)
(Base Case: MSL-8F_1DPV-72)

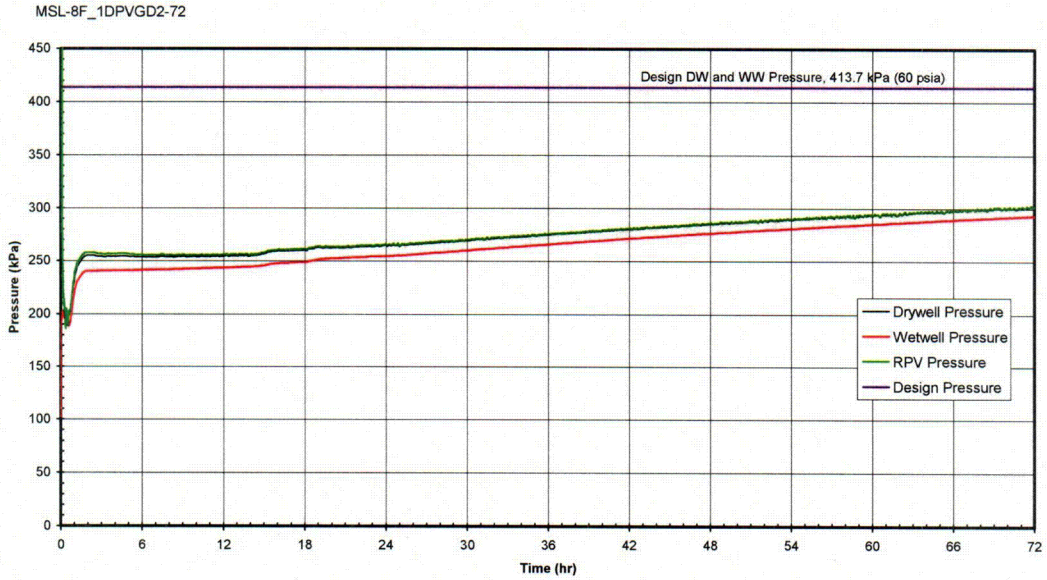

Figure 6.2-52_36 Containment Pressure Response
(Parametric Case: MSL-8F_1DPVGD2-72)

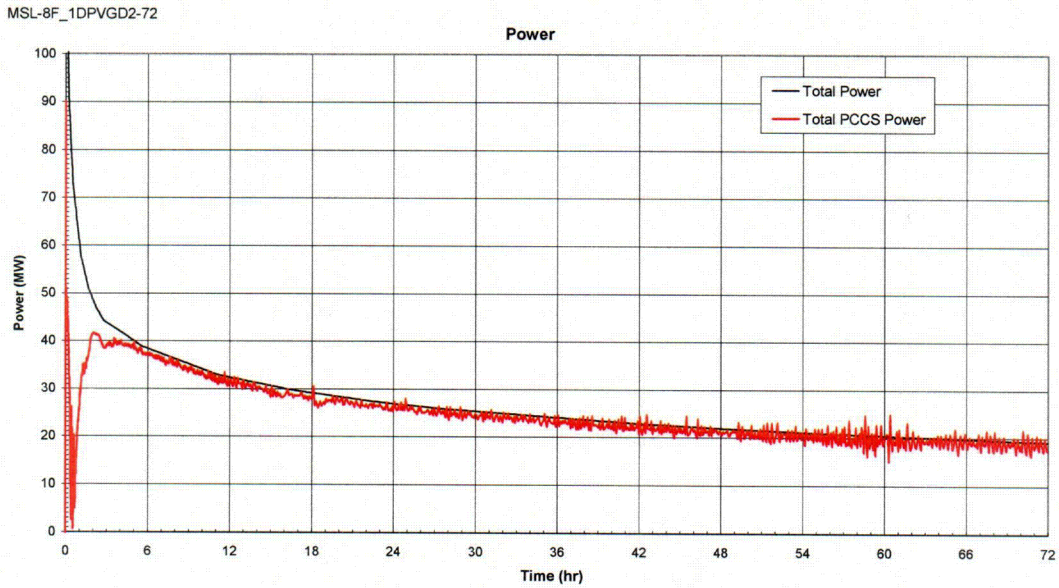

Figure 6.2-52_37 PCCS Heat Removal versus Decay Heat
(Parametric Case: MSL-8F_1DPVGD2-72)

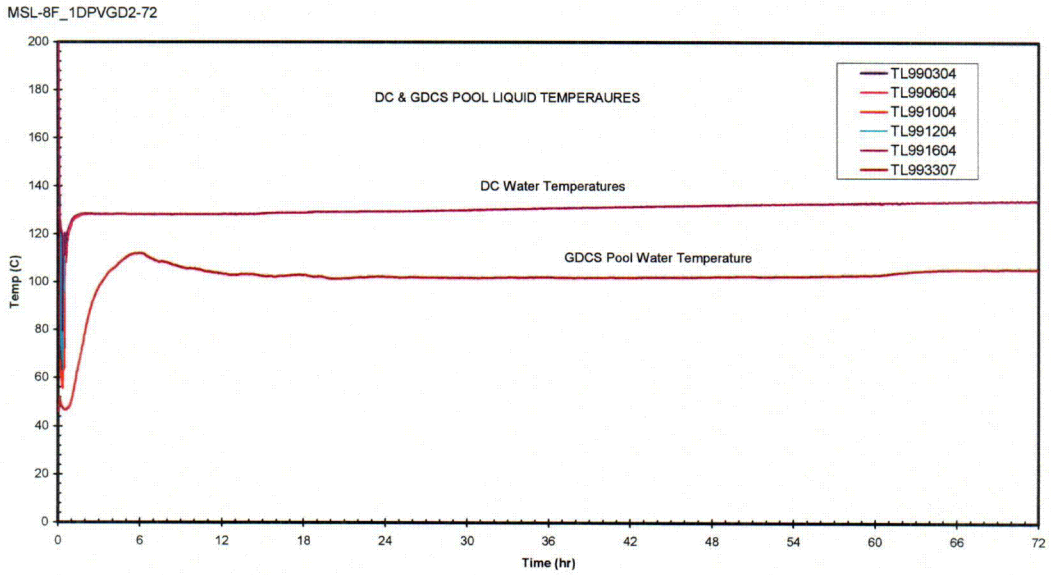

Figure 6.2-52_38 GDCS Pool Water Temperature

(Parametric Case: MSL-8F_1DPVGD2-72)

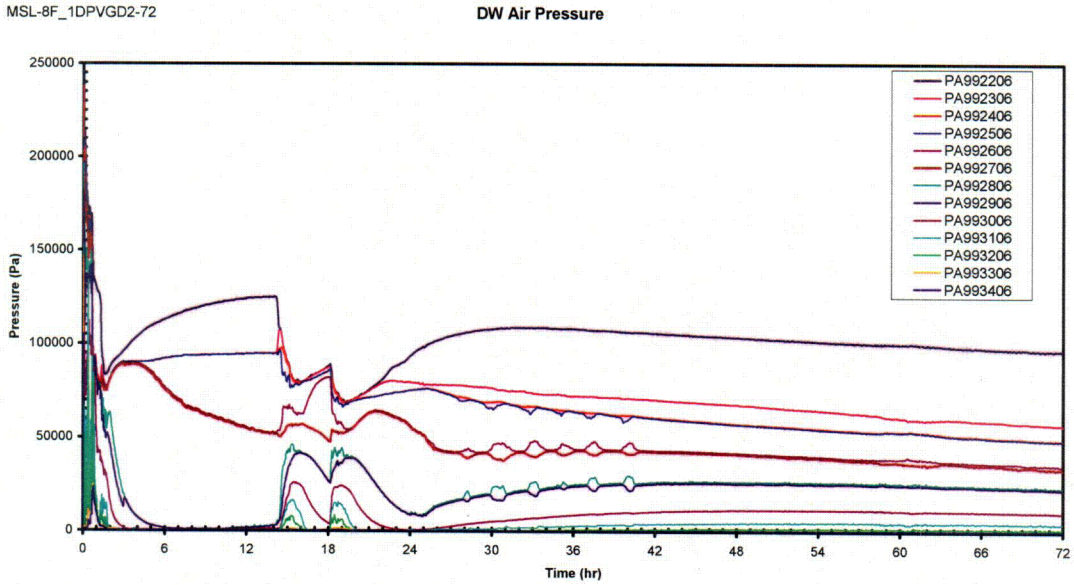

Figure 6.2-52_39 DW annulus NC Gas Pressure (Level 23=2nd level from DW Bottom, 34=Top)

(Parametric Case: MSL-8F_1DPVGD2-72)

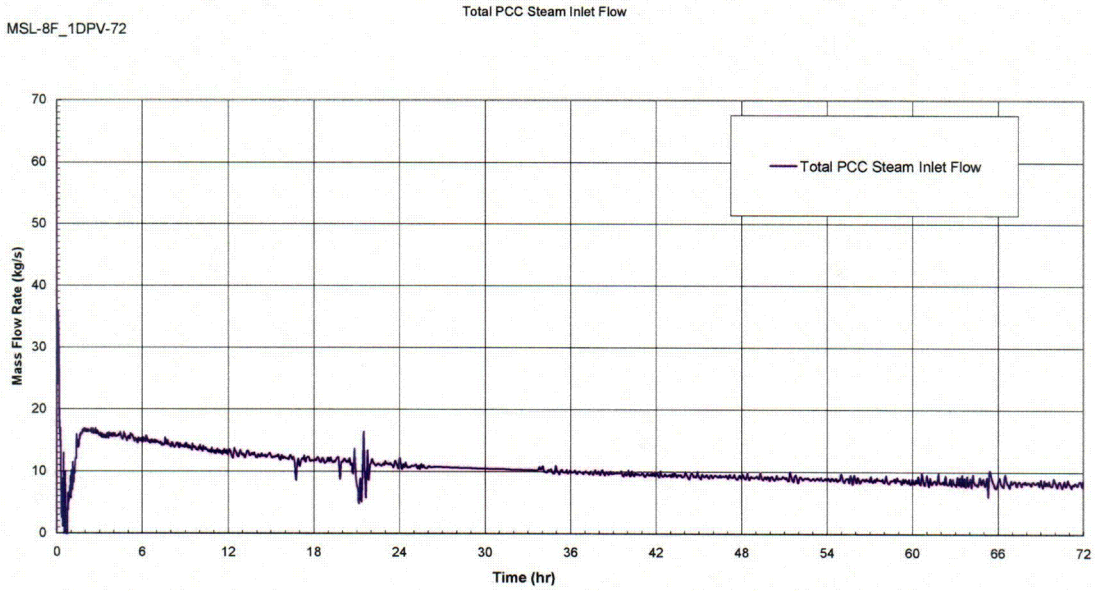

Figure 6.2-52_40 Total PCC Steam Inlet Flow
(Base Case: MSL-8F_1DPV-72)

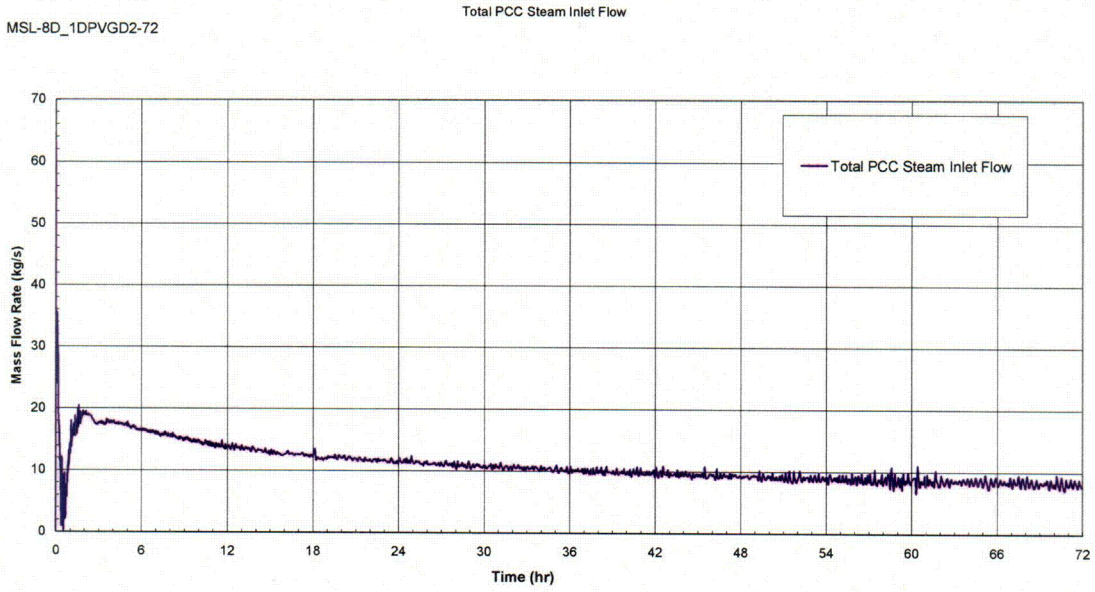

Figure 6.2-52_41 Total PCC Steam Inlet Flow
(Parametric Case: MSL-8F_1DPVGD2-72)

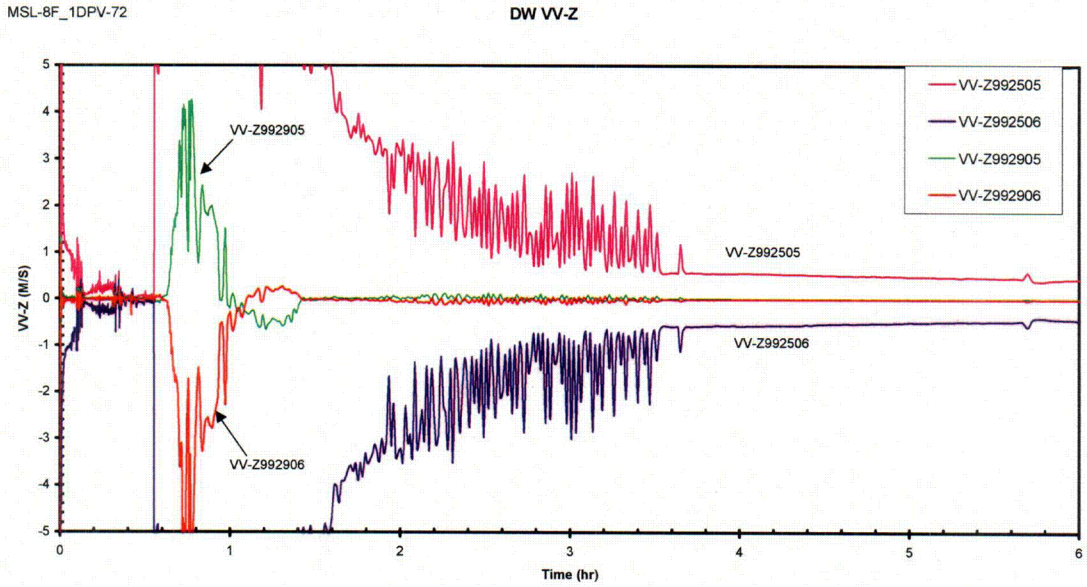

Figure 6.2-52 42 Vapor Velocities at Levels 25 and 29 in DW Annulus
(Base Case: MSL-8F_1DPV-72)

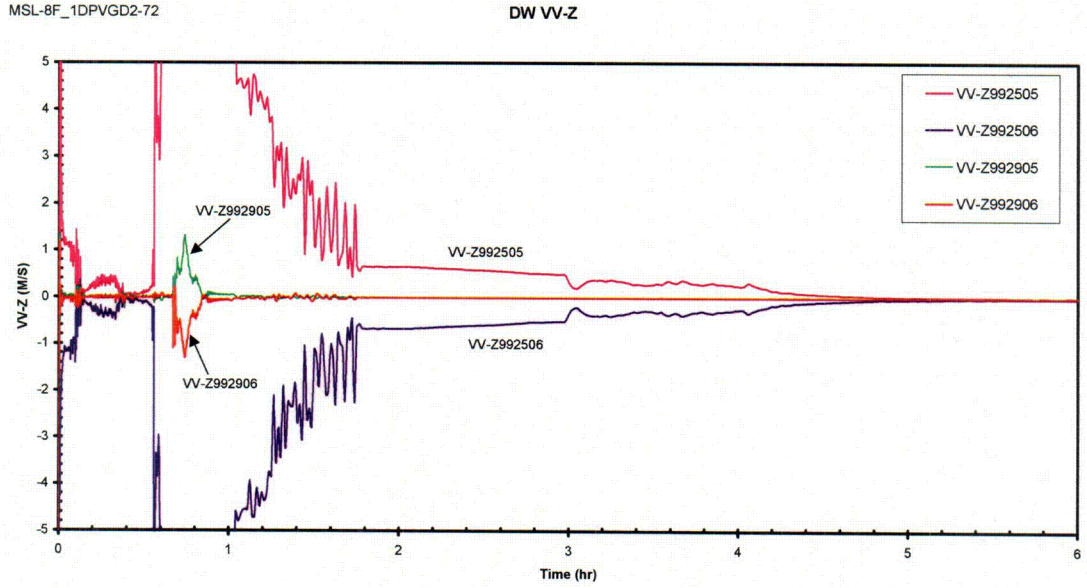

Figure 6.2-52 43 Vapor Velocities at Levels 25 and 29 in DW Annulus
(Parametric Case: MSL-8F_1DPVGD2-72)

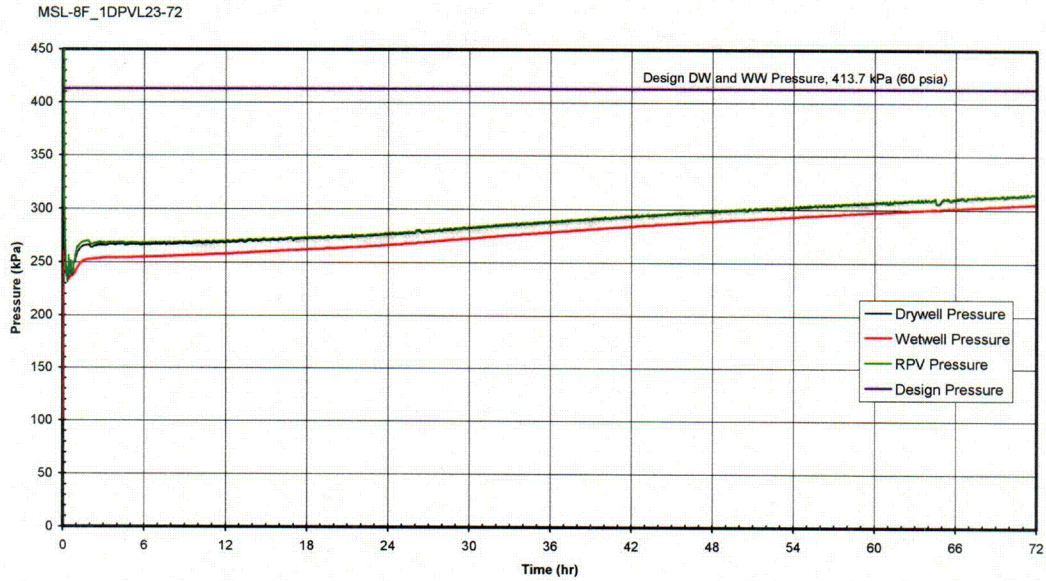

Figure 6.2-52_44 Containment Pressure Response
(Parametric Case: MSL-8F_1DPVL23-72)

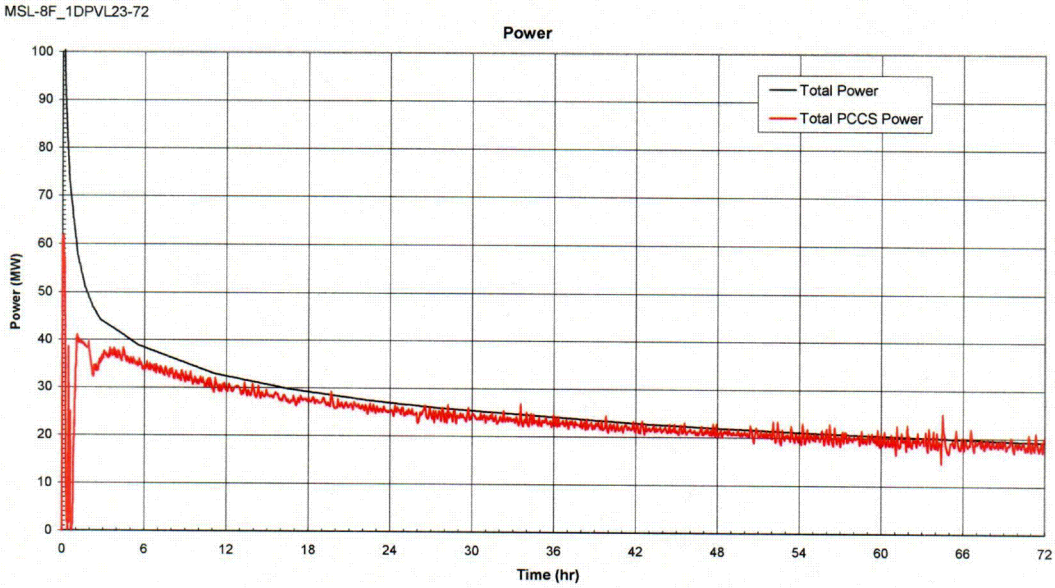

Figure 6.2-52_45 PCCS Heat Removal versus Decay Heat
(Parametric Case: MSL-8F_1DPVL23-72)

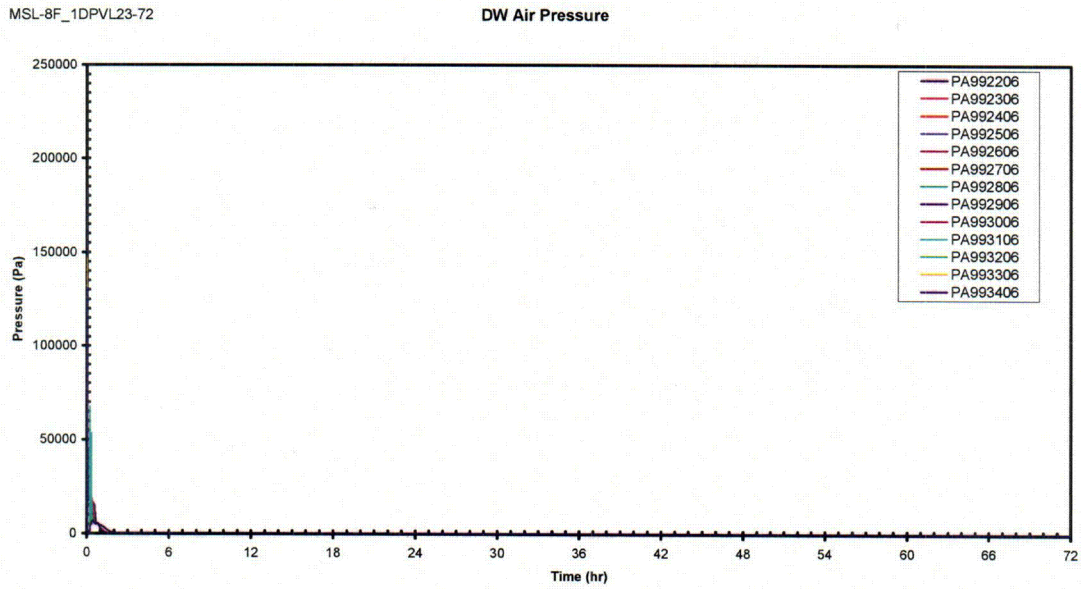

Figure 6.2-52 46 DW Annulus NC Gas Pressures (Level 22=Bottom, 34=Top)
(Parametric Case: MSL-8F_1DPVL23-72)

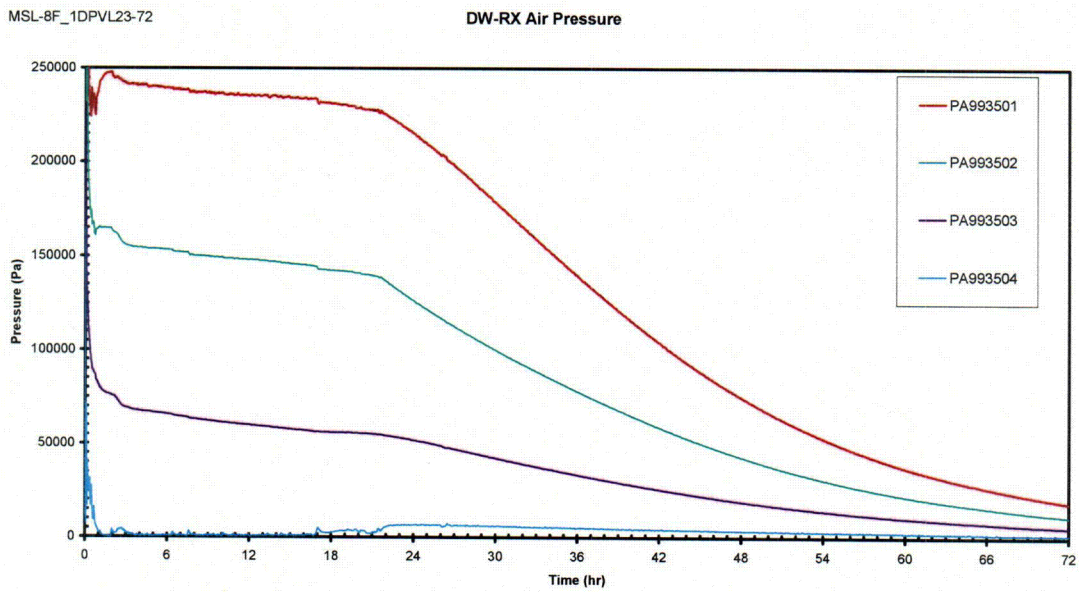

Figure 6.2-52 47 DW Head NC Gas Pressures (Level 35=Drywell Head)
(Base Case: MSL-8F_1DPVL23-72)

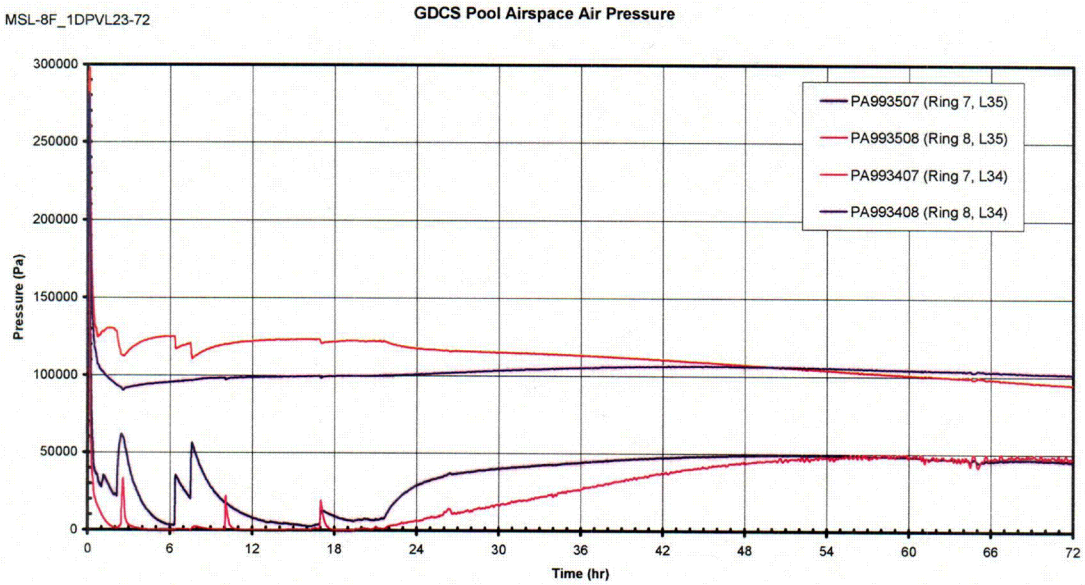

Figure 6.2-52 48 GDCS Pool Airspace NC Gas Pressures
(Base Case: MSL-8F_1DPVL23-72)

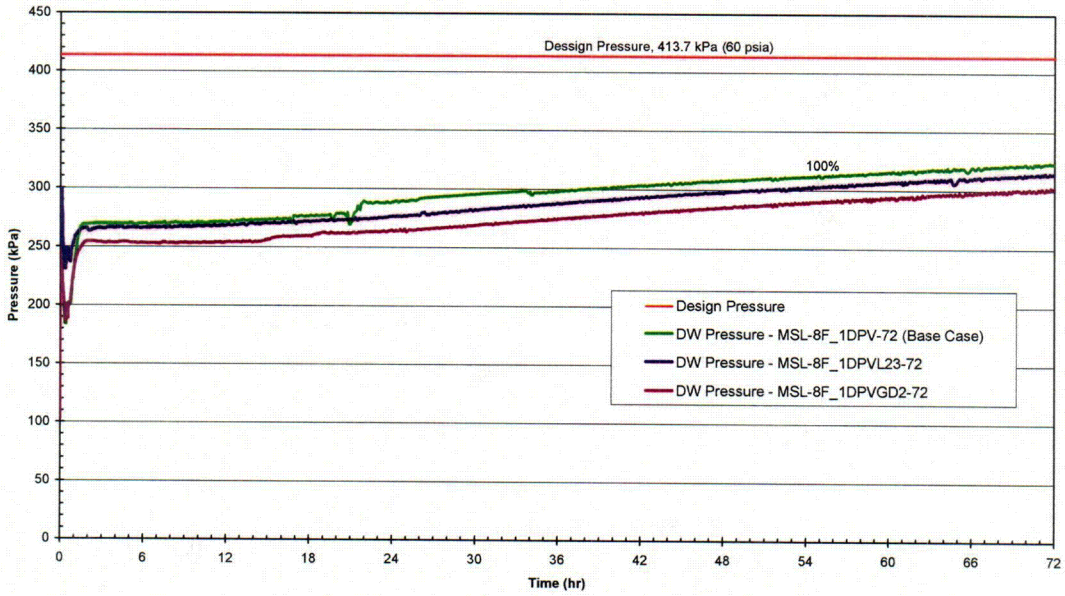

Figure 6.2-52 49 Comparison of DW Pressures – Base Case vs. Parametric Case

NRC RAI 6.2-58

For each break type (FWLB, MSLB, GDCS line, and bottom drain line) provide a discussion of the single failures considered and provide the resulting peak pressure and temperature for each case evaluated, in a tabular form, using appropriate licensing analysis assumptions to conservatively maximize the containment pressure or temperature response for each case. Include this information in the DCD Tier 2.

Response to RAI 6.2-58

DCD Rev. 1, Table 6.3-6 summarizes the single, active failures that are considered in the ECCS performance analysis. The assumed single failures are: one depressurization valve (DPV), one safety/relief valve (SRV), and one GDCS injection valve. Other postulated failures are not specifically considered, because they all result in at least as much ECCS capacity as one of the above failures.

For containment evaluation (except the feedwater line break), the peak containment pressure occurs at the long-term time period that is long after the first initiation of the SRVs and DPVs. After the opening of the DPVs, the long-term containment responses from different assumed single failure are expected to be similar. A single failure of one DPV is assumed in the long-term (72 hrs) containment analyses of main steam line break, GDCS line break, and bottom drain line break.

For the feedwater line break, results from the short-term ECCS analyses show that the peak DW pressure occurs shortly after the DPV opening and the case with 1 SRV failure generates higher short-term pressure than other single failures. A single failure of one SRV is assumed in the long-term (72 hrs) containment analysis of feedwater line break. In this feedwater line break analysis, the long-term DW pressure is lower than the first peak occurring shortly after the DPV opening.

The peak containment pressures for the each break type and assumed single failure with nominal conditions (Table 6.2-6, DCD Tier 2, Rev. 1) are summarized in Table 6.2-58_1. This table identifies that the main steamline break is the limiting break case for peak DW pressure. This break case will be analyzed using the bounding conditions (Table 6.2-6, DCD Tier 2, Rev. 1) to maximize the containment pressure. This bounding main steam line break case will be incorporated into the next DCD revision.

DCD Section 6.2.1.1.3 will be revised in a future update to include the above discussion and result.

Table 6.2-58_1 Summary of Peak DW Pressures Different Break Types (Nominal Conditions)

Break Type	Case ID	Max. DW Pressure (kPa)	Time at Max.
Main Steamline	MSL-8F_1DPV-72	323.0	71.7 hrs
Feedwater Line	FWL-8D_1SRV-72	306.2	77.8 sec
GDCS Line	GDL-8D_1DPV-72	276.6	391.1 sec
Bottom Drain Line	BDL-8D_1DPV-72	263.4	7.9 hrs